ABSTRACT

THE STABILITY OF PLANE POISEUILLE FLOW SUBJECT TO A TRANSVERSE MAGNETIC FIELD

Ву

James Anthony Kutchey

The stability of an electrically conducting fluid flowing between parallel planes subject to a transverse magnetic field is investigated for infinitesimal three-dimensional disturbances. Primary interest is in the effect of the magnetic field and magnetic fluid parameters on the critical point of the neutral stability curves. The governing stability equations include perturbations for both the velocity and magnetic fields and result in a sixth order coupled set of linear ordinary differential equations. This set represents an eigenvalue problem that is transformed to an initial value problem and solved numerically using a fourth order Runge-Kutta integration scheme with a special filtering technique.

The results indicate a strong dependence of the critical eigenvalues on both the magnetic field strength and a fluid property, the magnetic Prandtl number. The effect of both is to greatly stabilize the flow. Inclusion of the span-wise wave number does not affect the eigenvalues other than in a manner predicted by Squire's Theorem. The numerical results are also compared to previous data obtained by asymptotic expansion techniques.

THE STABILITY OF PLANE POISEUILLE FLOW SUBJECT TO A TRANSVERSE MAGNETIC FIELD

Ву

James Anthony Kutchey

A THESIS

Submitted to
Michigan State University
in partial fulfillment of the requirements
for the degree of

DOCTOR OF PHILOSOPHY

Department of Mechanical Engineering

1970

ACKNOW LEDGMENTS

2 - 6 5 -

The author wishes to express his sincere appreciation to his Major Professor, Dr. Merle C. Potter, Associate Professor of Mechanical Engineering for his valuable guidance and encouragement throughout this study. Without his personal interest and concern this thesis representing the consumation of the author's graduate work would not have been possible. Special thanks are conveyed to Dr. Charles R. St. Clair, Jr., Chairman, Mechanical Engineering Department for his advice and support in this graduate program.

Thankful acknowledgment is extended to other members of the Guidance Committee: Dr. James V. Beck, Dr. J.S. Frame, and Dr. K.M. Chen.

The author is grateful for financial support received from a NSF Traineeship and for supporting funds from the Mechanical Engineering Department and Division of Engineering Research.

To his wife, Arlene, the author dedicates this dissertation for her understanding, cooperation, and patience during the entire graduate program.

TABLE OF CONTENTS

			Page
	List	of Tables	v
	List	of Figures	vii
	Nome	nclature	viii
CHAPTER			
I.	INTRO	DDUCTION	1
	1.1 1.2	Review of Literature Description of the Problem	1 7
II.	STAB	ILITY EQUATIONS	9
	2.1	Fundamental Equations	9
	2.2	Non-Dimensional Variables	12
	2.4	Distributions	13
	4.4	Disturbances	15
	2.5	Eigenvalue Problem	18
III.	NUME	RICAL SOLUTION OF THE STABILITY EQUATIONS	19
	3.1	Introduction	19
	3.2	Starting Conditions	19
	3.3	Growth of the Eigenfunctions	20
	3.4	Purification Scheme	22
	3.5	Iteration Scheme for the Eigenvalues	25
	3.6	Criterion for Guessing the Eigenvalues	27
	3.7	Range of Parameters Considered	27
	3.8	Special Case of Zero Hartmann Number	28
IV.		LTS, CONCLUSIONS, AND RECOMMENDATIONS FOR HER STUDY	30
		·	
	4.1	Numerical Results	30
	4.2	Conclusions	33
	4.3	Recommendations for Further Study	34

BIBLIOGE	RAPHY	35
ILLUSTRA	ATIONS (Tables and Figures)	38
APPENDI	CES	
A	NUMERICAL TECHNIQUE TO SOLVE THE GOVERNING STABILITY EQUATIONS	58
В	COMPUTER PROGRAM	62
	B-1 Description of the Computer Program	62
	B-2 Listing of the Computer	02
	Program	64

LIST OF TABLES

Table		Page
1.	Comparison of Critical Eigenvalues	38
2.	Eigenvalues for the Stability Equations for the Case of Neutral Stability (c = 0.0) $M = 0.001$, $P_m = 10^{-6}$	39
3.	Eigenvalues for the Stability Equations for the Case of Neutral Stability ($c_i = 0.0$) $M = 1.0, P_m = 10^{-6}$	39
4.	Eigenvalues for the Stability Equations for the Case of Neutral Stability ($c_i = 0.0$) $M = 1.0, P_m = 10^{-1}$	40
5.	Eigenvalues for the Stability Equations for the Case of Neutral Stability (c = 0.0) $M = 2.0$, $P_m = 10^{-6}$	40
6.	Eigenvalues for the Stability Equations for the Case of Neutral Stability ($c_i = 0.0$) $M = 2.0, P_m = 10^{-1}$	41
7.	Eigenvalues for the Stability Equations for the Case of Neutral Stability ($c_1 = 0.0$) $M = 3.0, P_m = 10^{-6}$	41
8.	Eigenvalues for the Stability Equations for the Case of Neutral Stability (c = 0.0) $M = 3.0$, $P_m = 10^{-1}$	42
9.	Eigenvalues for the Stability Equations for the Case of Neutral Stability ($c_i = 0.0$) $M = 4.0$, $P_m = 10^{-6}$	42
10.	Eigenvalues for the Stability Equations for the Case of Neutral Stability (c. = 0.0) $M = 4.0$, $P_m = 10^{-1}$	43
11.	Eigenvalues for the Stability Equations for the Case of Neutral Stability (c. = 0.0) $M = 5.0$, $P_m = 10^{-6}$	43

12.	Eigenvalues for the Stability Equations for the Case of Neutral Stability (c. = 0.0) $M = 5.0$, $P_m = 10^{-1}$	44
13.	Eigenvalues for the Stability Equations for the Case of Neutral Stability (c _i = 0.0) M = 6.0, P _m = 10 ⁻⁶	44
14.	Eigenvalues for the Stability Equations for the Case of Neutral Stability (c = 0.0) $M = 6.0$, $P_m = 10^{-2}$	45
15.	Eigenvalues for the Stability Equations for the Case of Neutral Stability ($c_1 = 0.0$) $M = 6.0$, $P_m = 10^{-1}$	45

LIST OF FIGURES

Figure		Page
1.	Primary Flow Configuration	46
2.	Dimensionless Primary Velocity Profiles for Various Hartmann Numbers	47
3.	Wave Number α Versus Reynolds Number R for Neutral Stability for M = 0	48
4.	Wave Number α Versus Reynolds Number R for Neutral Stability for M = 1.0	49
5.	Wave Number α Versus Reynolds Number R for Neutral Stability for M = 2.0	50
6.	Wave Number α Versus Reynolds Number R for Neutral Stability for M = 3.0	51
7.	Wave Number α Versus Reynolds Number R for Neutral Stability for M = 4.0	52
8.	Wave Number α Versus Reynolds Number R for Neutral Stability for M = 5.0	53
9.	Wave Number α Versus Reynolds Number R for Neutral Stability for M = 6.0	54
10.	Plot of Eigenfunctions $\psi = \psi + i\psi$ at the Critical Point for $M = 0.001^r$	55
11.	Plot of Eigenfunctions $\psi = \psi_r + i\psi_i$ at the	
	Critical Point for $P_m = 10^{-6}$ and 10^{-1} for $M = 5.0$	56
12.	Plot of Eigenfunctions $\phi = \phi + i\phi_i$ at the Critical Point for $P_m = 10^{-6}$ and 10^{-1} for $M = 5.0$	57

NOMENCLATURE

a	Channel half width
^a 1, ^a 2, ^a 3	Coefficients used to obtain combined
	functions
$\vec{\mathtt{B}}$	Magnetic flux density
$c = c_r + ic_i$	Complex propagation speed of wave
c r	Wave speed
c _i	Amplification rate
$\vec{\mathtt{D}}$	Electric flux density
Ē	Electric field
F	Body force
मं	Applied magnetic field with com-
	ponents $(H_x, H_y, 0)$
\vec{h}	Magnetic perturbations with com-
	ponents (h_x, h_y, h_z)
j	Conduction current
$\kappa^2 = \alpha^2 + \beta^2$	Square of combined wave number
М	Hartmann number = $\mu \text{Ha} \left(\frac{\sigma}{\rho \nu}\right)^{\frac{1}{2}}$
[™] e	Magnetization vector
\vec{P}	Polarization vector
P _{in}	Magnetic Prandtl number = $v_{\mu\sigma}$
p	Pressure
R	Reynolds number = $\frac{U_{m}}{M}$
ΔR	Change in R

R _m	Magnetic Reynolds number = $U_{m}^{a\mu\sigma}$
t	Time
Т	Test function
U _m	Average velocity
₹	Primary velocity with components
	(U, 0, 0)
\vec{v}	Velocity perturbations with com-
	ponents (v_x, v_y, v_z)
x, y, z	Coordinate axes
α	Wave number in flow direction
Δα	Change in α
β	Spanwise wave number
σ	Electrical conductivity
μ	Magnetic permeability
€	Permittivity (dielectric constant)
ρ _e	Space charge density
ជ	Vorticity of primary flow = $\nabla \times \vec{V}$
Ē	Vorticity of perturbed flow = $\nabla \times \vec{v}$
ρ	Mass density of fluid
ν	Kinematic viscosity of fluid
Φ	Complex eigenfunction for magnetic
	perturbations
¥	Complex eigenfunction for velocity
	perturbations
▽	Del operator = $i \frac{\partial}{\partial x} + j \frac{\partial}{\partial y} + k \frac{\partial}{\partial z}$
v ²	Del operator = $i \frac{\partial}{\partial x} + j \frac{\partial}{\partial z} + k \frac{\partial}{\partial z}$ Laplacian = $\frac{\partial}{\partial x} + \frac{\partial}{\partial z} + \frac{\partial}{\partial z} + \frac{\partial}{\partial z}$

Step size = Δy Δ Superscripts () Differentiation with respect to y (,) Differentiation with respect to time ()* Dimensional quantities Magnitudes of perturbation quantities Subscripts ()_w Quantities at wall ()_p Primary flow and magnetic quantities

CHAPTER I

INTRODUCTION

1.1 Review of Literature

The term "transition" as generally used in the field of fluid mechanics applies to the observable change in flow pattern when well-ordered laminar motion becomes turbulent. The theory of stability using perturbation techniques with an assumed form of infinitesimal disturbances attempts to predict the value of the critical Reynolds number or point of instability for a prescribed main flow.

The earliest work in the area of transition was performed by Reynolds (1883) when he used dye injection for flow in pipes. Theoretical studies to predict the transition from laminar to turbulent flow were begun by Lord Rayleigh (1880, 1887) and Lord Kelvin (1887). Based upon this work, independent studies by Orr (1907) and Sommerfeld (1908) led to the now well known Orr-Sommerfeld stability equation for two-dimensional flow, which is given by

$$(U-c)(\phi'' - \alpha^2 \phi) - U'' \phi = -\frac{i}{\alpha R} (\phi^{iv} - 2 \alpha^2 \phi'' + \alpha^4 \phi)$$

where U = Velocity

c = Complex wave propagation speed

 α = Wave number

ø = Eigenfunction

R = Reynolds number

This equation is based upon the assumption of infinitesimal periodic distrubances.

Neglecting the effects of viscosity, Lord Rayleigh (1914) was able to show that any velocity profile that possesses an inflection point is unstable. Much later, Tollmein (1935) proved that this was not only a necessary but sufficient condition for the amplification of small disturbances.

Prandt1 (1914) postulated the existence of a viscous boundary layer and was able to define transition, separation and drag coefficients on bodies. Incorporating the viscous boundary layer into stability theory, Prandt1 (1921) considered flow over a flat plate and included the effects of the largest viscous terms near the wall. This work along with calculations performed by Tietjens (1925) gave the startling result that the introduction of viscosity into the equations did not produce damping as was presumed but amplification for sufficiently large Reynolds numbers for particular wavelengths of the disturbances.

must be taken into account not only near the wall but also in the critical layer. The critical layer is a narrow region surrounding the critical point at which the main flow velocity and the wave propagation velocity are equal, that is, U = c. In addition, he also showed that the influence of viscosity leads to instability only if the main flow velocity profile is other than a straight line.

The method developed by Tollmein, based on Asymptotic Theory, provided the mathematical basis for later progress in the stability area. Lin (1945, 1946, 1955) was able to provide a firm mathematical basis for the asymptotic expansion theory and was able to explain the nature of the functions near the critical point. He discussed what he called the inner viscous layer which includes the critical point, and the outer viscous layer, a wall viscous layer.

The asymptotic expansion method was used almost exclusively until the advent of modern high-speed digital computers which permit the use of more accurate numerical techniques. Even now, however, the asymptotic method can be effectively used to predict the type of functional behavior to be expected, prior to obtaining numerical solutions.

The stability of plane Poiseuille flow was investigated by Thomas (1953) with a numerical scheme. He obtained a value for the minimum Reynolds number, R_{crit}, for neutral stability of 5780, which is based on maximum channel velocity and the half-width. This value has been shown to be more accurate than Lin's (1945) value of 5300 or Stuart's (1954) value of 5100 based on asymptotic techniques.

Potter (1965) studied the stability of plane Couette-Poiseuille flow by asymptotic expansions and later (1967) performed numerical calculations for symmetrical parabolic flows. The values obtained for $R_{\rm crit}$ were in close agreement with those of Thomas.

The point of instability as determined theoretically and the physically observable transition point from laminar to turbulent flow often differ considerably. An explanation for these differences was thought by some to be due to the fact that the derivation of the Orr-Sommerfeld equation is based on the assumption of two-dimensional disturbances only. Squire (1933) showed that if three-dimensional disturbances are considered the flow is more stable, that is, a higher value of R_{crit} is predicted, than for two-dimensional disturbances.

The distance between the point of instability and the actual transition point depends upon the degree of amplification present and the intensity of fluctuations present in the primary flow. Schlichting (1933) performed calculations for boundary layer flow over a flat plate and investigated the parameters in the interior of the neutral stability curve (C_i > 0) to help explain the actual mechanism of disturbance amplification. More recently, Shen (1954) repeated Schlichting's calculations, and Stuart (1956) investigated the amplification of unstable disturbances by accounting for the effect of the non-linear terms in the equations. Reynolds and Potter (1967) considered the instabilities of channel flow for disturbances of finite amplitude.

Except for early pipe flow measurements by Barnes and Coker (1905) and Ekman (1910), who succeeded in maintaining laminar flow for fairly high Reynolds numbers (40,000), experimental verification of the results of stability theory was slow in coming. Rosenbrook (1937) found agreement with

the inflexion point theorem due to Rayleigh and Tollmein.

Some of the most significant experimental work was performed by Schubauer and Skramstad (1947) and Dryden (1947) who performed very precise measurements for boundary layer flow over a flat plate (with very low free stream fluctuations), and showed the influence of free stream disturbance intensity on the critical Reynolds number.

Emmons (1951) observed that any disturbance which triggers transition may be "local in time" and once initiated, the turbulent spot moves downstream growing steadily in all directions. This phenomenom was studied by Schubauer-Klebanoff (1956).

Transition from laminar to turbulent flow in a boundary layer is now believed to take place within 4 stages. At the first stage, infinitesimal two dimensional waves called Tollmein-Schlichting waves, begin to amplify and become unstable. The two dimensional waves become three dimensional and result in hairpin eddies at the second stage. In the third stage low speed turbulent streaks or bursts (Emmons' spots) originate near the wall, and finally in the fourth stage the burst rate becomes constant and the transition to fully turbulent motion is completed. Morkovin (1958) reviews some of the recent advances in the study of transition and discusses the mechanisms involved in the above mentioned stages.

Stability theory yields a critical Reynolds number that corresponds to stage one. Since the third stage is the first point at which large scale variations take place, this is often

considered to be transition by many engineers. These differences along with the slower response times of earlier instrumentation serve to explain some of the discrepancies between
theory and experiment.

Stability predictions in channel flow yield critical Reynolds numbers that also correspond to infinitesimal disturbances but the stages of transition are not as apparent as in boundary layer flow. Free steam disturbances or disturbances which result from wall roughness amplify and lead to the transition described above but the effect is now propagated throughout the flow and the entire channel becomes turbulent.

In the area of magnetohydrodynamics (MHD), the velocity and magnetic field equations for an incompressible, viscous and electrically conducting fluid moving in the presence of a magnetic field have been derived by Batchelor (1950). The effect of a magnetic field on thermal instabilities was investigated independently by Thompson (1951) and Chandrasekhar (1952). For a complete discussion of this problem and others in the field of hydrodynamic and hydromagnetic stability the reader is referred to Chandrasekhar (1961).

Stuart (1954) considered the stability of viscous flow between parallel planes in the presence of a co-planar magnetic field. Lock (1956) investigated a similar problem but considered the effect of a magnetic field perpendicular to both the confining parallel planes and the flow direction. Both Stuart and Lock simplified the resulting sixth order set of equations and solved the fourth order Orr-Sommerfeld equation

by asymptotic expansions. To simplify the analysis, Lock utilized Squire's theorem, as detailed by Michael (1953) for the case of MHD flows.

1.2 Description of the Problem

The purpose of the present study is to investigate the stability of an electrically conducting fluid flowing between parallel planes subject to the influence of a transverse magnetic field. The coordinate system is oriented with the origin at the centerline, the x-axis in the direction of the flow and the y-axis perpendicular to the bounding plates as shown in figure 1. The planes are assumed to be non-conducting and located at $y = \pm a$.

The governing equations, developed in the next chapter result in a coupled set of ordinary linear differential equations, a fourth order equation on ψ , the velocity perturbation, and a second order equation on ϕ the magnetic field perturbation.

The above problem was considered by Lock in 1956. He had to make several simplifying assumptions in order to obtain a solution by asymptotic expansions. The reduced equation that he solved was the following modified Orr-Sommerfeld equation:

$$(U-c)(\psi'' - \alpha^2 \psi) - U''\psi = -\frac{i}{\alpha R} \psi^{iv}$$
 (1.2.1)

where the only effect of the magnetic field is to modify the primary velocity profile U(y).

The eigenvalues that appear in most stability equations normally occur in the combinations of $(\alpha^2 + \beta^2)$, αR , and c_r , and thus, Squire's Theorem is applicable. In the governing coupled equations for this problem α appears in the magnetic equation as a separate coefficient indicating that the solutions may be subject to an influence of β , the spanwise (z-direction) component of the disturbance wave. Chawla (1969) in studying the effect of rotation on the stability of flow over a flat plate, found that the rotational effects were directly coupled to β and Squire's Theorem was not applicable. Although Lock initially assumed three-dimensional disturbances, his simplifying assumptions delete the magnetic equation and he is then justified in applying Squire's Theorem.

This study provides a solution of the complete set of stability equations for various magnetic quantities and fluid properties and also provides bounds for which Lock's assumptions are justified.

CHAPTER II

STABILITY EQUATIONS

2.1 Fundamental Equations

Consider first the interaction of the electric and magnetic fields which are given by Maxwell's equations. These equations written for a non-relativistic reference frame are

$$\nabla \cdot \vec{D} = \rho_{\rho} \tag{2.1.1}$$

$$\nabla \cdot \vec{B} = 0 \tag{2.1.2}$$

$$\nabla \times \vec{E} = -\vec{B} \tag{2.1.3}$$

$$\nabla \times \vec{H} = \vec{J} + \dot{\vec{D}}$$
 (2.1.4)

where \vec{D} = Electric flux density

 \vec{E} = Electric field

 \vec{B} = Magnetic flux density

H = Magnetic field

 ρ_{e} = Space charge density

 \vec{J} = Conduction current density

and the notation (') implies $\frac{\lambda}{\lambda t}$, t being time.

In addition to these equations, the current conservation equation

$$\nabla \cdot \vec{J} + \dot{\rho}_e = 0 \tag{2.1.5}$$

is often used; although, it is not independent of Maxwell's equations and follows directly from (2.1.1) and (2.1.4).

The conduction current is given by Ohm's Law

$$\vec{J} = \sigma(\vec{E} + \vec{V} \times \vec{B}) - \rho_e \vec{V}$$
 (2.1.6)

where σ is the electrical conductivity, and \vec{V} is the velocity vector.

The constitutive equations for a linear medium are

$$\vec{D} = \varepsilon \vec{E} + \vec{P} \tag{2.1.7a}$$

$$\vec{B} = \mu(\vec{H} + \vec{M}_e) \qquad (2.1.7b)$$

where the polarization \vec{P} and magnetization \vec{M}_e vectors can be neglected for conducting fluids; μ is the magnetic permeability and ϵ is the permittivity, also known as the dielectric constant.

For most materials, and in particular for all conducting liquids and gases μ is that of free space μ_0 . The assumption that $\epsilon = \epsilon_0$, however, can be used only for plasmas, but by using the current conservation equation (2.1.5) this assumption need not be made.

Following the procedure outlined by Chandrasekhar (1961) some simplifications can now be made to arrive at the equations generally used to solve MHD flow problems. The assumptions are:

- 1. The non-relativistic approximation has already been stated and is consistent with the Newtonian form of the equations of motion that will be used.
- 2. Without an externally applied electric field, the electric fields originate only from the induced effects and are of the same order of magnitude as $\vec{V} \times \vec{B}$ appearing in

Ohm's Law.

- 3. High frequency phenomena are not considered so that the displacement current \overrightarrow{D} is neglected in equation (2.1.4) compared to \overrightarrow{J} , the conduction current. In fact for metals, the displacement current is meaningless and need not be mentioned.
- 4. In Ohm's Law, which determines the conduction current, the space charge ρ_e may be neglected. For liquid conductors and in dense, collision-dominated plasmas, which may be treated by a continuum model as an ordinary conducting gas, the space charge effects become unimportant. Ohm's Law is then written as

$$\vec{J} = \sigma(\vec{E} + \vec{V} \times \vec{B}) \tag{2.1.8}$$

where it is further assumed that the conductivity is constant with frequency and independent of the magnetic field.

The small electric field and the negligible displacement current imply the main interaction is between the magnetic field and the fluid, hence the magnetohydrodynamics.

The Navier-Stokes equations governing the motion of an incompressible fluid are

$$\vec{\vec{V}} + (\vec{\vec{V}} \cdot \nabla)\vec{\vec{V}} = \frac{1}{\rho} \nabla p + \nu \nabla^2 \vec{\vec{V}} + \frac{1}{\rho} \vec{F}$$
 (2.1.9)

where the body force term is $\vec{F} = \vec{J} \times \vec{B}$, p is the pressure, p is the mass density and ν is the kinematic viscosity. The equation of continuity is

$$\nabla \cdot \vec{V} = 0 . \tag{2.1.10}$$

The equations now relevant to the problem are:

Maxwell's equations

$$\nabla \cdot \vec{H} = 0 \tag{2.1.11}$$

$$\nabla \times \vec{H} = \vec{J} \tag{2.1.12}$$

$$\nabla \times \vec{E} = -\mu \vec{H} \qquad (2.1.13)$$

Ohm's law:
$$\vec{J} = \sigma(\vec{E} + \vec{V} \times \mu \vec{H})$$
 (2.1.14)

Continuity:
$$\nabla \cdot \vec{V} = 0$$
 (2.1.15)

Navier-Stokes:

$$\vec{\vec{v}} + (\vec{v} \cdot \nabla)\vec{\vec{v}} = \frac{\mu}{\rho} (\vec{J} \times \vec{H}) - \frac{1}{\rho} \nabla p + \nu \nabla^2 \vec{v} \qquad (2.1.16)$$

Eliminating the electric field \vec{E} between equations (2.1.13) and (2.1.14), together with (2.1.12) leads to the magnetic equation

$$\vec{H} - \nabla \times (\vec{V} \times \vec{H}) = \frac{1}{\mu \sigma} \nabla^2 \vec{H}$$
 (2.1.17)

This equation along with (2.1.15), (2.1.16) and (2.1.12) are sufficient to determine all the variables, \vec{V} , \vec{H} , and p.

2.2 Non-Dimensional Variables

To write the equations in non-dimensional form, choose the average velocity \mathbf{U}_{m} , the channel half width (a) and the applied magnetic field strength \mathbf{H}_{O} as reference quantities. The dimensionless variables will then be

$$\vec{V} = \frac{\vec{V}_{m}^{*}}{\vec{V}_{m}} \qquad x_{i} = \frac{x_{i}^{*}}{\vec{a}}$$

$$t = \frac{U_{m}t^{*}}{\vec{a}} \qquad p = \frac{p}{\rho U_{m}^{2}}$$

$$\vec{H} = \frac{\vec{H}_{o}^{*}}{\vec{H}_{o}} \qquad \vec{J} = \frac{\vec{J}_{a}^{*}}{\vec{H}_{o}}$$

$$(2.2.1)$$

where $x_i \Rightarrow (x, y, z)$ the cartesian coordinates, and the asterisks denote the previously used dimensional quantities.

Introducing these in the governing equations yields

$$\vec{\mathbf{v}} + (\vec{\mathbf{v}} \cdot \nabla)\vec{\mathbf{v}} = -\nabla \mathbf{p} + \frac{1}{R} \nabla^2 \vec{\mathbf{v}} + \frac{M^2}{RR_m} (\vec{\mathbf{J}} \times \vec{\mathbf{H}})$$
 (2.2.2)

$$\vec{H} - \nabla \times (\vec{V} \times \vec{H}) = \frac{1}{R_{m}} \nabla^{2} \vec{H}$$
 (2.2.3)

$$\vec{J} = \nabla \times \vec{H} \tag{2.2.4}$$

$$\nabla \cdot \vec{H} = 0 \tag{2.2.5}$$

$$\nabla \cdot \vec{V} = 0 \tag{2.2.6}$$

where R = Reynolds number = $\frac{U_m a}{V_m}$

 $M = Hartmann number = \mu Ha(\frac{\sigma}{\rho \nu})^{\frac{1}{2}}$

 $R_{\rm m}$ = Magnetic Reynolds no. = $U_{\rm m}a~\mu\sigma$

It should be noted here that the above dimensionless groups are not unique and that others may be formed by multiplying togehter various combinations of the above. One such parameter that will be used later is the magnetic Prandtl number $P_m = v\mu\sigma = \frac{R}{R} \ .$

2.3 The Primary Flow and Magnetic Field Distributions

The solution for steady, two-dimensional motion of a conducting fluid between parallel planes subjected to a

transverse magnetic field is well known and has been provided by Hartmann and Lazarus (1937). For parallel flows, the velocity components are (U, 0, 0) and for this problem the magnetic field has the components $(H_x, H_y, 0)$, all functions of y only.

Equation (2.2.3) yields

$$\frac{1}{R_{\rm m}} \frac{d^2 H_{\rm x}}{dy^2} = -\frac{d}{dy} (UH_{\rm y})$$
 (2.3.1)

and

$$\frac{d^2 H}{dy^2} = 0 {(2.3.2)}$$

Since the normal component of $\mu \vec{H}$ must be continuous and have the same value at both walls and since the applied magnetic field induction is in the y direction, equation (2.3.2) shows that H_y is a constant H. This result can also be obtained from equation (2.2.5) which represents continuity of the magnetic field.

Differentiating the x-component of (2.2.2) with respect to y yields

$$\frac{M^{2}}{R_{m}} \frac{d^{2}H}{dy^{2}} = \frac{d^{3}U}{dy^{3}}$$
 (2.3.3)

Eliminating H_x between (2.3.1) and (2.3.3) results in

$$\frac{d^3U}{dy} = M^2 \frac{dU}{dy}$$
 (2.3.4)

The solution to the above equation is

$$U = \frac{M(\cosh M - \cosh My)}{M \cosh M - \sinh M}$$
 (2.3.5)

		•

İ

For zero magnetic fields, this equation should reduce to the standard parabolic profile, $U = 1.5 \, (1-y^2)$. This is found to be the case when the first two terms of the series expansions are substituted for the hyperbolic functions.

To determine the induced magnetic field in the direction of flow, substitute equation (2.3.5) into (2.3.3). The resulting equation and the boundary conditions that H_{χ} must be zero at both walls since there is no applied magnetic field in this direction yields

$$H_{x} = \frac{R_{m} \text{ (sinh My - y sinh M)}}{M(\cosh M-1)}$$

2.4 The Linearized Equations for Small Disturbances

The primary velocity and magnetic field quantities are now considered to have superimposed on them three-dimensional infinitesimal disturbances. They are then written

$$\vec{V} = \vec{V}_p + \vec{V}$$

$$\vec{H} = \vec{H}_p + \vec{h}$$
(2.4.1)

where
$$\vec{v}_p \Rightarrow (U, 0, 0)$$

 $\vec{H}_p \Rightarrow (H_x, H_y, 0)$
 $\vec{v} \Rightarrow (v_x, v_y, v_z)$
 $\vec{h} \Rightarrow (h_x, h_y, h_z)$

Substituting (2.4.1) into equation (2.2.3), subtracting off the original equation for the primary flow and neglecting the squares of all the disturbance quantities yields

$$\dot{\vec{h}} = (\vec{H}_p \cdot \nabla) \vec{v} + (\vec{h} \cdot \nabla) \vec{V}_p - (\vec{V}_p \cdot \nabla) \vec{h} - (\vec{v} \cdot \nabla) \vec{H}_p + \frac{1}{R_m} \nabla^2 \vec{h} \qquad (2.4.2)$$

The pressure gradient term is first eliminated from the momentum equation by taking the curl of both sides. The disturbance equation is then found as above, and the vorticity equation for the perturbations results.

$$\vec{\xi} + (\vec{V}_p \cdot \nabla) \vec{\xi} + (\vec{V} \cdot \nabla) \vec{\Omega}_p = (\vec{\Omega}_p \cdot \nabla) \vec{V} + (\vec{\xi} \cdot \nabla) \vec{V}_p + \frac{1}{R} \nabla^2 \vec{\xi}$$

$$+ \frac{M^2}{RR_m} \left\{ (\vec{H}_p \cdot \nabla) \vec{j} + (\vec{h} \cdot \nabla) \vec{J}_p - (\vec{J}_p \cdot \nabla) \vec{h} - (\vec{j} \cdot \nabla) \vec{H}_p \right\} \qquad (2.4.3)$$
where $\vec{\Omega}_p = \text{vorticity of main flow} = \nabla \times \vec{V}_p$

$$\vec{\xi} = \text{vorticity of perturbed flow} = \nabla \times \vec{V}$$

$$\vec{J}_p = (\nabla \times \vec{H}_p)$$

$$\vec{i} = (\nabla \times \vec{h})$$

In addition, the following continuity equations result

$$\nabla \cdot \vec{v} = 0 \tag{2.4.4}$$

$$\nabla \cdot \vec{h} = 0 \tag{2.4.5}$$

Consider further that the assumed three-dimensional disturbances take the separated form

$$\mathbf{v}_{\mathbf{x}} = \hat{\mathbf{v}}_{\mathbf{x}}(\mathbf{y}) \exp[\mathbf{i}(\alpha \mathbf{x} + \beta \mathbf{z}) - \mathbf{i}\alpha \mathbf{c}t]$$

$$\mathbf{v}_{\mathbf{y}} = \psi(\mathbf{y}) \exp[\mathbf{i}(\alpha \mathbf{x} + \beta \mathbf{z}) - \mathbf{i}\alpha \mathbf{c}t]$$

$$\mathbf{v}_{\mathbf{z}} = \hat{\mathbf{v}}_{\mathbf{z}}(\mathbf{y}) \exp[\mathbf{i}(\alpha \mathbf{x} + \beta \mathbf{z}) - \mathbf{i}\alpha \mathbf{c}t]$$

$$\mathbf{h}_{\mathbf{x}} = \hat{\mathbf{h}}_{\mathbf{x}}(\mathbf{y}) \exp[\mathbf{i}(\alpha \mathbf{x} + \beta \mathbf{z}) - \mathbf{i}\alpha \mathbf{c}t]$$

$$\mathbf{h}_{\mathbf{y}} = \phi(\mathbf{y}) \exp[\mathbf{i}(\alpha \mathbf{x} + \beta \mathbf{z}) - \mathbf{i}\alpha \mathbf{c}t]$$

$$\mathbf{h}_{\mathbf{z}} = \hat{\mathbf{h}}_{\mathbf{z}}(\mathbf{y}) \exp[\mathbf{i}(\alpha \mathbf{x} + \beta \mathbf{z}) - \mathbf{i}\alpha \mathbf{c}t]$$

The assumed form of the disturbances implies a spatially periodic wave with complex amplitudes where α and β are dimensionless wave numbers and are real quantities. The complex

wave speed c is given by

$$c = c_r + ic_i$$
 (2.4.7)

where c_i is the amplification rate. A positive or negative c_i implies growth or decay respectively of the perturbations. This study is concerned with neutral stability, that is, $c_i = 0$.

Introducing the assumed form of the disturbances into the component form of equations (2.4.2) and (2.4.3) and then eliminating $\mathbf{v}_{\mathbf{x}}$, $\mathbf{v}_{\mathbf{z}}$, $\mathbf{h}_{\mathbf{x}}$, and $\mathbf{h}_{\mathbf{z}}$ with a procedure similar to that outlined by Chawla or Stuart (1954), yields the following

$$h\psi - \frac{i\psi'}{\alpha} = (U-c)\phi + \frac{i}{\alpha R_{m}} (\phi'' - K^{2}\phi) \qquad (2.4.8)$$

$$(U-c)(\psi'' - K^{2}\psi) - U''\psi + \frac{i}{\alpha R} (\psi^{iv} - 2K^{2}\psi'' + K''\psi)$$

$$= P\{h(\phi'' - K^{2}\phi) - \frac{i}{\alpha} (\phi''' - K^{2}\phi^{\dagger}) - h''\phi\}$$

$$\text{where } h = H_{x} = \frac{R_{m} (\sinh My - y \sinh M)}{M (\cosh M - 1)}$$

$$U = \frac{M (\cosh M - \cosh My)}{M \cosh M - \sinh M}$$

$$K^{2} = \alpha^{2} + \beta^{2}$$

$$P = \frac{M^{2}}{RR}$$

and primes indicate differentiation with respect to y.

Equations (2.4.8) and (2.4.9) can be solved simultaneously or can be combined to form a single sixth order equation. Combining the equations requires tedious algebra and the resulting coefficients are extremely long and unwieldy.

No insight or simplification is gained by such a combination

so that it is better to solve the two equations simultaneously.

The necessary boundary conditions result from the noslip velocity conditions at the wall and from continuity, namely,

$$\psi = \psi' = 0$$
 @ $y = \pm 1$

and the nature of the magnetic field perturbations (2.4.10)

$$\phi = 0$$
 @ y = + 1

The problem is now completely specified.

2.5 Eigenvalue Problem

The system of equations and boundary conditions derived above, represent an eigenvalue problem with the characteristic values α , β , c, R and M. The wave propagation speed, c as stated earlier is complex, with the imaginary part being the exponential growth or decay rate of the assumed disturbances. Since neutral stability curves are desired c_i is set to zero.

To solve for the characteristic values it is necessary to specify some of them, say M, β and c and solve for the remaining two, namely α and R from equations (2.4.8) and (2.4.9).

The neutral stability curve (α vs. R for constant M) will have a minimum R, called the critical Reynolds number R_{crit} , for which a disturbance is neutrally stable. Reynolds numbers greater than R_{crit} result in growth for that particular disturbance and Reynolds numbers smaller than R_{crit} result in decay. Associated with R_{crit} there is also a critical wave speed (c_r) and a critical wave number

CHAPTER III

NUMERICAL SOLUTION OF THE STABILITY EQUATIONS

3.1 Introduction

The numerical solution to equations (2.4.8) and (2.4.9) will generate three independent solutions because the solutions are started at one wall with three boundary conditions already satisfied. These solutions cannot each satisfy all of the boundary conditions at both walls. However, a proper linear combination of these functions will yield the total eigenfunction which must then satisfy the three boundary conditions at the opposite wall.

The integration of the equations is begun at the lower wall (y = -1) and proceeds step by step across the channel to the upper wall. A fourth order Runge-Kutta technique, detailed in appendix A is used to solve the equations. The three independent solutions are each initialized at the lower wall and integrated simultaneously at each step across the channel.

3.2 Starting Conditions

To use the Runge-Kutta integration scheme to solve a differential equation of order n the problem must be transformed to an initial value problem where the function and its n-l derivatives are initially specified. For equations

(2.4.8) and (2.4.9), the boundary conditions (2.4.10) provide starting values for ψ_i , ψ_i^{\dagger} and ϕ_i (i=1,2,3 and represent the separate solutions) with values for the remaining derivatives ψ_i^{\dagger} , ψ_i^{\dagger} and ϕ_i^{\dagger} somewhat arbitrary. The highest order derivatives, namely ψ_i^{\dagger} and ϕ_i^{\dagger} , do not require initialization since they are determined in terms of the lower order derivatives.

The "arbitrary" starting conditions mentioned above must be chosen so as to insure independent functions, at least at the start of the integration. A purification scheme maintains independence as the integration proceeds. Assigning a non-zero value to one of the three unspecified derivatives for each of the three solutions should help keep the solutions linearly independent. Specifically $\psi_2^{"}$, $\psi_3^{"}$, and $\phi_1^{"}$ are given non-zero values.

The purification scheme requires identification of the fastest growing solution. This was accomplished by checking the ratio of $\frac{\psi_i^i}{\psi_i}$ at the first integration step for each of the independent solutions. The values obtained for i=1, 2, 3 were approximately 400, 300, and 200 respectively and, as should be expected, were unaffected by the relative magnitudes of the starting values assigned to ψ_2^{ii} , ψ_3^{iii} and ϕ_1^{ii} .

3.3 Growth of the Eigenfunctions

It is well known that during the numerical integration one of the two independent functions for the fourth order problem and at least one of the three independent functions for the sixth order problem grows very rapidly. Kaplan (1964) referred to these functions as the "growing solutions" and called the others the "well behaved solutions". The growing solutions stem from the viscous portion of the stability equations and the well behaved functions originate from the inviscid portion.

The governing stability equations can be written as

$$[h\psi - \frac{i}{\alpha}\psi' - (U-c)\phi] = \frac{i}{\alpha R_{m}} [\phi'' - K^{2}\phi]$$

$$[(U-c)(\psi'' - K^{2}\psi) - U''\psi] = \frac{i}{\alpha R} [\psi^{iv} - 2K^{2}\psi'' + K^{4}\psi$$

$$- \frac{i\alpha M^{2}}{R_{m}} \{h(\phi'' - K^{2}\phi) - \frac{i}{\alpha} (\phi'''' - K^{2}\phi') - h''\phi\}]$$

$$(3.3.1)$$

The terms in the square brackets on the left hand side represent the inviscid part and those in the brackets on the right hand side the viscous part.

In this particular problem, for the larger Hartmann numbers and magnetic Prandtl numbers the three solutions exhibited three distinct growth rates, which could be termed the largest growing solution, intermediate growing solution and the well behaved solution. As an example, for the case of M=4.0 and $P_m=10^{-1}$ the three functions exhibited growths across the channel on the order of 10^{280} , 10^{140} and 10^6 respectively. This extreme growth limited the range of Hartmann numbers that could be considered in this study as it is apparent that the limitations of the computer are soon exceeded.

For M = 0 (.001 for the computer program) the equations effectively reduce to fourth order and result in only one growing solution which exhibited a growth on the order of

		,
		,
		,
		,

10³⁶ across the channel, which is in agreement with the observations reported by Reynolds and Potter (1967).

The final combined solution, of course, does not exhibit this rapid growth which indicates that only a very small portion of the growing solutions are required to form the eigenfunctions.

3.4 Purification Scheme

The very rapid growth rate exhibited by some of the solutions causes some difficulties other than machine over-flow.

Initially all three solutions are linearly independent but as the integration proceeds, this independence is observed to disappear rapidly. Kaplan (1964) states that this loss of independence, which is impossible for an exact solution, arises because of the approximate nature of the numerical integration. Errors are introduced because any numerical method being applied at small but finite steps has associated with it a truncation error and in addition a digital computer carries only a fixed number of digits, resulting in round off error. Kaplan further concludes that the arbitrary initial conditions for the well-behaved solution contain a small portion that is also an initial condition for the growing solutions. As the integration proceeds it grows much more rapidly than the behaved solution and soon dominates it. Even if this small portion is not present initially, it is effectively introduced by truncation errors.

Kaplan's conclusions appear justified although the actual mechanism that causes one solution to "pollute" the other may be open to question.

The goal is, therefore, to keep the solutions independent over as large a range as possible. To reduce the truncation error associated with any numerical scheme, an obvious answer is to choose a step size that is as small as possible consistent with the particular limitations of machine storage and speed. Performing all arithmetic operations in double precision should greatly reduce the round-off error. This is in fact, found to be true. However, since all the functions are complex, adding double precision to the program significantly increases machine computation time and storage requirements.

Kaplan suggests an alternate approach that does not require double precision, namely, a filtering technique. His method consists of subtracting from the well-behaved solution a portion of the growing solution at every step of the integration. This procedure called "filtering" prevents the growing solution from ever dominating the well-behaved solution and thus maintains the needed functional independence.

Kaplan's shoeme was implemented in the computer program for this problem. The CDC 6500 computer nominally carries about 15 significant digits in single precision, which is equivalent to double precision on IBM equipment and in particular the IBM 7090 used by Kaplan. These computations were in effect then performed in "double precision". In fact, for the cases with Hartmann number equal to zero or one no suppression

scheme was required. Test cases of M = 2 or 3 revealed that Kaplan's scheme was required. For M > 3 however, the scheme was no longer sufficient to maintain independence. In this range the growth becomes very large, and the second solution becomes an intermediate growing solution which now pollutes the well-behaved solution. A double suppression scheme suggested by W. Reynolds of Stanford in a private communication to M. Potter was used to find the two remaining solutions.

The filter used consisted of a ratio of the inviscid solutions (left hand side of equation (3.3.2)), namely,

where, (inviscid)
$$m = i\alpha R[(U-c)(\psi_m'' - K^2\psi_m) - U''\psi_m]$$
 (3.4.2)
 $m = 1, 2, 3$

The above ratio determines the fraction of the growing solution to be "extracted" from the behaved solution, so the amount subtracted off is the product of this ratio and the value of the growing solution at the particular integration step. This product was equal to about 20% of the behaved solution.

The final scheme consisted of extracting from solutions two and three a portion of the fastest growing solution (one) and then extracting from solution three a portion of the intermediate growing solution (two). Once incorporated this method assured complete independence of the three separate solutions for all growth rates even to the point of exceeding the overflow limits of the machine.

3.5 Iteration Scheme for the Eigenvalues

Integrating across the channel, three independent solutions are generated at each step. Upon reaching the opposite wall, the functions are linearly combined to form the total eigenfunctions that must satisfy the boundary conditions. The three conditions that must be satisfied are $\psi = \psi' = \phi = 0$. Consider the following set of combined functions at the wall:

$$a_1\psi_1 + a_2\psi_2 + a_3\psi_3 = \psi_{\omega}$$
 (3.5.1)

$$a_1\psi_1^{\dagger} + a_2\psi_2^{\dagger} + a_3\psi_3^{\dagger} = \psi_w^{\dagger}$$
 (3.5.2)

$$a_1 \psi_1'' + a_2 \psi_2'' + a_3 \psi_3'' = \psi_w''$$
 (3.5.3)

$$a_1 \phi_1 + a_2 \phi_2 + a_3 \phi_3 = \Phi_{u}$$
 (3.5.4)

Equations (3.5.2-4) are used to solve for the coefficients \mathbf{a}_i . Note that there is no specific boundary condition for $\psi_W^{"}$, hence the choice here is arbitrary. As long as ψ_W is non-zero, the value assumed merely changes the normalization factor and still represents a valid solution. This system can now be written as

$$\begin{bmatrix} \psi_1' & \psi_2' & \psi_3' \\ \psi_1'' & \psi_2'' & \psi_3'' \\ \phi_1 & \phi_2 & \phi_3 \end{bmatrix} \begin{bmatrix} a_1 \\ a_2 \\ a_3 \end{bmatrix} = \begin{bmatrix} 0 \\ 1 \\ 0 \end{bmatrix}$$

For functions that are linearly independent the determinant of the matrix containing known values of ψ' , ψ'' and ϕ will be non-zero. When the double suppression scheme, discussed in the previous section, was not used this determinant

was effectively zero and indicated the functions to be linearly dependent, that is, one column is a multiple or combination of the other two.

For independent functions, the a_i can be determined by finding the inverse of this matrix or as was done for the computer program by simply writing out the solution.

The a_i , once determined can now be substituted into equation (3.5.1). With the correct eigenvalues ψ_w will be zero; hence ψ_w will serve as the test function (T). If $T \times (\text{conjugate } T)$ is less than 10^{-12} the convergence criteria is satisfied and the eigenvalues used to generate the functions are assumed to be the correct ones. If convergence is not attained let $T_1 = T$. Increase α by 1%, recalculate T and let $T_2 = T$. After setting α to its original value, increase R by 1%, calculate T and let $T_3 = T$. The finite difference approximations for the change in T with respect to α and R are

$$\frac{\Delta T}{\partial \alpha} \approx \frac{T_2 - T_1}{\Delta \alpha} \tag{3.5.5}$$

$$\frac{\partial T}{\partial R} \approx \frac{T_3 - T_1}{\Delta R} \tag{3.5.6}$$

These are substituted into the complex equation

$$\frac{\Delta T}{\delta^{\alpha}} \Delta_{\alpha} + \frac{\Delta T}{\delta R} \Delta R + T_{1} = 0 \qquad (3.5.7)$$

from which $\Delta \alpha$ and ΔR can be calculated. The new values for the eigenvalues are

$$\alpha_{\text{new}} = \alpha_{\text{old}} + \Delta \alpha$$

$$R_{\text{new}} = R_{\text{old}} + \Delta R$$
(3.5.8)

It is apparent that for every iteration or new "guess" of eigenvalues the equations must be integrated across the channel three times. It was found that if the initial guesses are relatively good, convergence is obtained in about three iterations.

3.6 Criterion for Guessing the Eigenvalues

The initial estimates for some of the eigenvalues were obtained from the data presented by Lock (1954). Where his data was not applicable (M > 3, $P_{\rm m} = 10^{-1}$), guesses had to be made with extreme care. Hopefully, the iteration process would iterate to the correct eigenvalues, although this did not always occur because of the small radius of convergence. After a few points were obtained and plotted, the next estimates could be obtained by extrapolation until the complete stability curve was generated.

3.7 Range of Parameters Considered

Hartmann numbers in the range of zero to six were run for magnetic Prandtl numbers (P_m) of 10^{-6} and 10^{-1} . Test cases for magnetic Prandtl numbers less than 10^{-6} were run with no change in eigenvalues. Physically, Prandtl numbers in the range of 10^{-6} to 10^{-4} are characteristic of liquid metals and it was hoped that the study could be extended to $P_m = 100$, which is characteristic of ionized gases. At these values,

however, the functional growth rates became excessive, resulting in machine overflow.

As an example of the large variations associated with a change in P_m refer to the case of M = 6 as plotted in Figure 9. Included on this figure is a neutral stability curve for $P_m = 10^{-2}$ in addition to 10^{-6} and 10^{-1} . The change in R_{crit} for $P_m = 10^{-6}$ to 10^{-2} is only about one-ninth the change from 10^{-2} to 10^{-1} . It is apparent then that a further increase of only one order of magnitude with its corresponding increase in functional growth rates soon puts the values out of manchine range.

Several values of β were tried at different Hartmann numbers and magnetic Prandtl numbers but, as will be discussed in the next chapter, no β -effect was found to exist except that predicted by Squire's Theorem.

3.8 Special Case of Zero Hartmann Number

The general equations are sixth order, but for the case of zero magnetic field the equations reduce to the standard fourth order Orr-Sommerfeld equation. Rather than write a separate computer program to solve this case it was felt that if the general program could be used it would provide a better check on proper program operation.

Hopefully, then, as M approaches zero the program should yield the known results for plane Poiseuille flow. This was found to be the case when M was set equal to 10^{-2} or 10^{-3} , with the same eigenvalues resulting for either value. A small

value was necessary since setting M equal to zero exactly yields an indeterminate result (0/0) in the calculation of the primary velocity profile. It also results in a reduction in the order of the equations thereby causing an indeterminate result when satisfying the boundary conditions.

CHAPTER IV

RESULTS, CONCLUSIONS, AND RECOMMENDATIONS FOR FURTHER STUDY

4.1 Numerical Results

Prior to obtaining any points on the stability curves, the subroutine which calculates the primary velocity profile and induced magnetic field quantities was run as a separate program. The non-magnetic case, as was discussed in the previous chapter was run at $M=10^{-3}$. The results of this run were compared to the parabolic profile for plane Poiseuille flow and found to agree to within at least five significant numbers. This profile along with others for M>0 are well known, see for example, the original work by Hartmann and Lazarus (1937) or any current textbook on MHD. Dimensionless plots of these curves are presented in Figure 2.

The data generated for the neutral stability curves are presented in Tables 2 through 15 and are also plotted along with Lock's data in Figures 3 through 9. A summary of the critical wave numbers and Reynolds numbers from this study and from Lock's data are presented in Table 1. Typical eigenfunctions are plotted in Figures 10, 11 and 12.

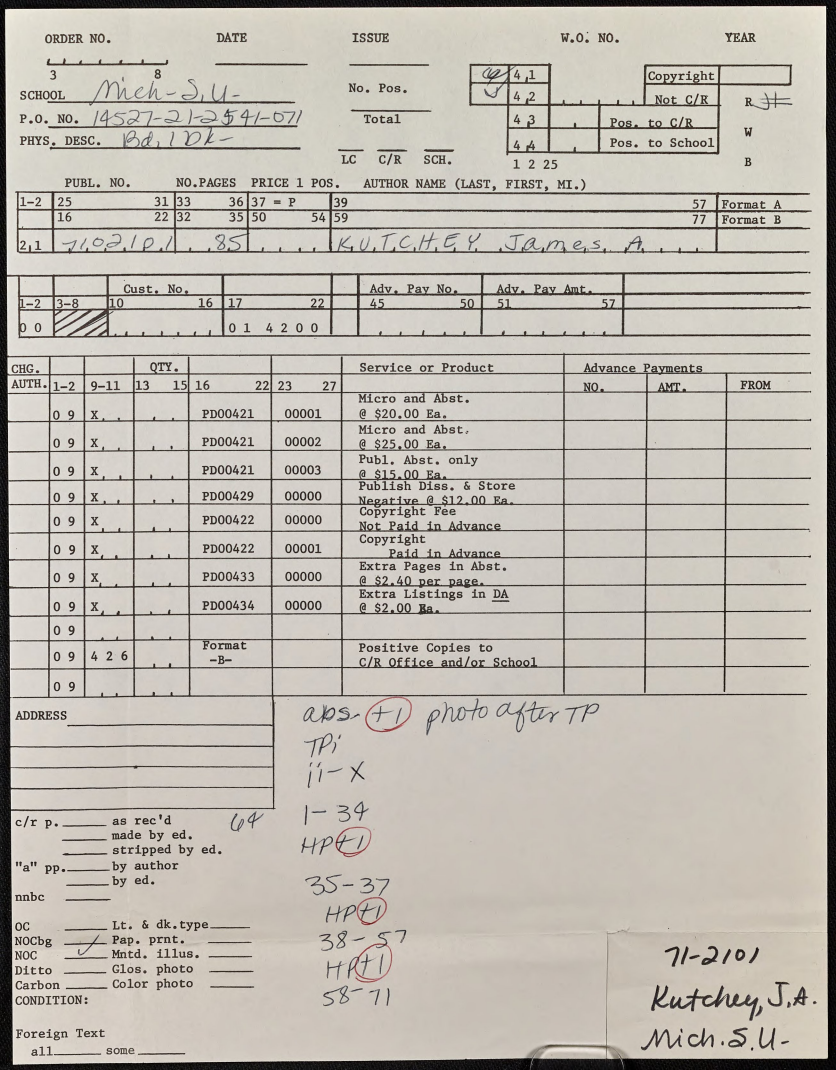
To reduce the equations to a form that could be solved by asymptotic expansions, Lock, based upon Stuart's paper (1954), used the assumption that for most conducting liquids, the magnetic Prandtl number P_m (= $R_m/R = v\mu\sigma$) is small. Provided therefore, that R is not too large, R_m will be small compared with unity. He then neglected the magnetic effects and reduced the sixth order set of equations to the following fourth order, modified Orr-Sommerfeld equation which he then solved:

$$(U-c)(\psi'' - \alpha^2 \psi) - U''\psi = -\frac{i}{\alpha R} \psi^{iv}$$
 (4.1.1)

In reducing the problem to this form, the only effect of the magnetic field is to modify the primary velocity profile.

Comparison of Lock's data as presented along with the present data is surprisingly good. For $P_m = 10^{-6}$ his critical points are a little high for M = 0 and 1, agree almost exactly at M = 2 and for $M \ge 3$ are low compared to this study. As M increases the deviations increase, which indicates a greater dependence of the solutions on the magnetic terms of equations (2.4.8) and (2.4.9) that were neglected by Lock.

As discussed in the problem description, an examination of the equations indicates that β , the spanwise component of the disturbance wave, should affect the final eigenvalues such that Squire's Theorem is not applicable. This was not found to be the case, however. The term $\frac{i}{\alpha}\psi$ ' in equation (2.4.8) that leads to this conclusion does not significantly affect the final solution. This was verified by several runs for various values for M and P_m with a non-zero (0.5) value of β , all of which produce the same eigenvalues as the $\beta=0$



case.

The influence of increasing Hartmann number is, of course, to stabilize the flow. For a given Hartmann number, a further stabilization of the flow occurs with an increase in the magnetic Prandtl number. These effects are presented graphically in Figures 3 through 9. Consider, for example, the case of M = 5.0 which is depicted in Figure 8. The critical Reynolds number increases from 132300 to 169400 for $P_m = 10^{-6}$ and 10^{-1} respectively. This increase due to the change in P_{m} stems from the fact that the eigenfunctions for the velocity perturbations ψ and the magnetic field perturbations ϕ at $P_m = 10^{-1}$ are now of the same order of magnitude. Hence, for this range the magnetic terms in the stability equations significantly affect the final eigenvalues. The magnitudes and behavior of the eigenfunctions for this case are shown in Figures 11 and 12 where we and do are plotted respectively. The & curves have been normalized to 1+0i at the centerline as is commonly done in the current literature.

Figure 9, which presents data for M=6.0 includes in addition to the neutral stability curves for $P_m=10^{-6}$ and 10^{-1} a curve for $P_m=10^{-2}$. The shift in $R_{\rm crit}$ for a change in P_m from 10^{-6} to 10^{-2} is only about 6000, from 169500 to 175800, but a value of $P_m=10^{-1}$ significantly increases $R_{\rm crit}$ to a value of 230700, indicating the large influence of the magnetic terms in the stability equations.

As discussed in Chapter III the growth rates of the independent eigenfunctions increase rapidly with increasing Hartmann number and magnetic Prandtl number. The growth rates with this numerical scheme become so large for M > 6 or $P_{\rm m} > 10^{-1} \quad {\rm that \ machine \ overflow \ occurs \ and \ no \ data \ could \ be}$ obtained. This phenomenon is evidently also due to the ϕ eigenfunctions.

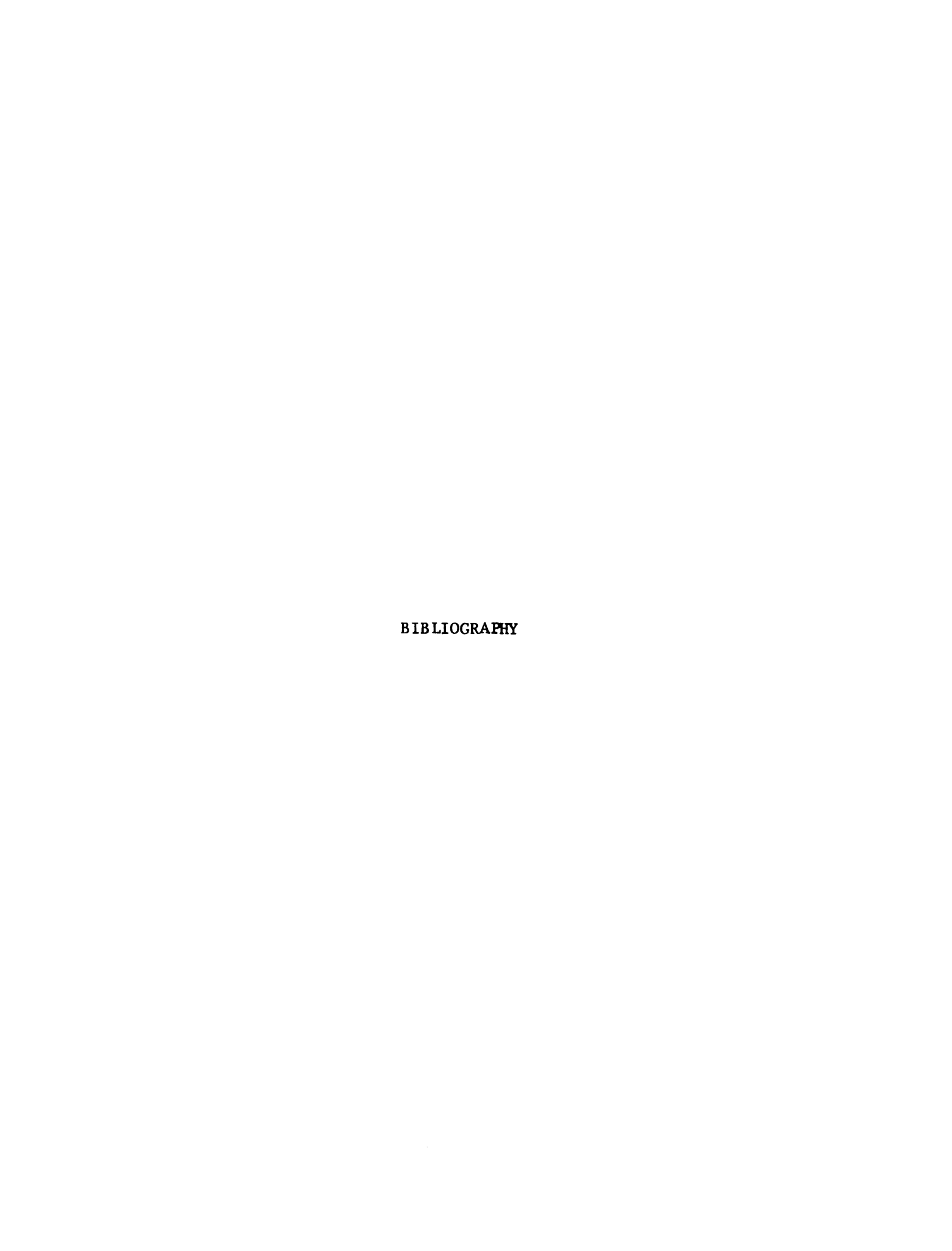
4.2 Conclusions

Based on the results obtained and the preceding discussion it can be concluded that for small magnetic Prandtl numbers (10⁻⁶) characteristic of liquid metals the standard Orr-Sommerfeld equation along with the modified velocity profile gives satisfactory results in determining neutral stability. For other conducting liquids or gases where the magnetic Prandtl is larger, the effects of the magnetic field must be fully accounted for. The effect of an increasing magnetic field strength is to greatly stabilize the flow and also to increase the critical wave number causing the instability.

Squire's Theorem is applicable to this problem since β does not affect the solutions, and K^2 which equals $\alpha^2 + \beta^2$ can be replaced by γ^2 in equations (2.4.8) and (2.4.9).

4.3 Recommendations for Further Study

This study could be further generalized to include conducting non-newtonian fluids which would include liquid metal amalgams, uranium slurries, seeded polymers, and others. The effects of geometry changes such as a finite channel with conducting side walls that would lead to different boundary conditions on the magnetic field could also be studied. Also of interest would be an investigation to compare the results of this study with stability curves obtained for $c_i \neq 0$.



BIBLIOGRAPHY

- Barnes, H. T. and Coker, E. G., "The Flow of Water Through Pipes". Proc. Roy. Soc. London, A 74, 341 (1905).
- Batchelor, G. K., "On the Spontaneous Magnetic Field in a Conducting Liquid in Turbulent Motion". Proc. Roy. Soc. London, A 201 (1950).
- Chandrasekhar, S., "On the Inhibition of Convection by a Magnetic Field". Phil. Mag. Ser. 7 43, (1952).
- Chandrasekhar, S., "Hydrodynamic and Hydromagnetic Stability". Clarendon Press (1961).
- Chawla, M. D., "The Stability of Boundary Layer Flow Subject to Rotation". Doctoral Dissertation, Michigan State University (1969).
- Collatz, L., "Numerische Behandlung von Differentialgleichungen". Springer-Verlag, Berlin (1951).
- Dryden, H.L., "Some Recent Contributions to the Study of Transition and Turbulent Boundary Layers". NACA TN 1168 (1947). Also, "Recent Advances in the Mechanics of Boundary Layer Flow". Adv. Appl. Mech. I, Academic Press (1948).
- Ekman, V. W., "Archiv fur Math". Astr. och Fys. VI, No. 12 (1910).
- Emmons, H. W., "The Laminar-Turbulent Transition in a Boundary Layer". Part I, <u>Journal of Aeronautical</u> Sciences, 18 (1951).
- Hartmann, J. and Lazarus, F., Math.-fys. Medd. 15 (1937).
- Kelvin, Lord, Philosophical Magazine. 5th Series t. xxiv (1887).
- Lin, C. C., "On the Stability of Two-Dimensional Parallel Flows". Part I, II, III, Quart. Appl. Math. 3, (1945, 1946).
- Lin, C. C., "The Theory of Hydrodynamic Stability". Cambridge University Press, London (1955).

- Lock, R. C., "The Stability of the Flow of an Electrically Conducting Fluid Between Parallel Planes under a Transverse Magnetic Field". Proc. Royal Soc. A 233 (1956).
- Michael, D. H., "Stability of Plane Parallel Flows of Electrically Conducting Fluids". Proc. Camb. Phil. Soc. 49. (1953).
- Morkovin, M. V., "Transition from Laminar to Turbulent Shear Flow A Review of Some Recent Advances in its Understanding". Trans. ASME. (1958).
- Orr, W. M'F., "The Stability or Instability of the Steady Motions of a Perfect Liquid and of a Viscous Liquid". Proc. Roy. Irish Academy, (A) 27 (1907-09).
- Potter, M. C., "The Stability of Plane Couette-Poiseuille Flow". Doctoral Dissertation, University of Michigan (1965). Later published in <u>J. Fluid Mech. (3)</u>, 24 (1966).
- Potter, M. C., "Linear Stability of Symmetrical Parabolic Flows". The Phy. of Fluids (3), 10 (1967).
- Prandtl, L. P., "Uber den Luftwiderstand von Kugeln".

 <u>Gottinger Nachrichter</u> (1914).
- Prandtl, L. P., "Bemerkungen Uber die Entstehung der Turbulenz". ZAMM, 1 (1921), and Phys. Z., 23 (1922).
- Rayleigh, Lord, "On the Stability or Instability of Certain Fluid Motions". Proc. Lond. Math. Soc., 11, 57 (1880) and 19, 67 (1887).
- Rayleigh, Lord, "Further Remarks on the Stability of Viscous Fluid Motion". Phil. Mag. and Journal of Science, 6 Series, 28 (1914).
- Reynolds, O., "An Experimental Investigation of the Circumstances which determine whether the Motion of Water shall be Direct or Sinous, and of the Law of Resistance in Parallel Channels". Phil. Trans. Roy. Soc. (1883).
- Reynolds, W. C. and Potter, M. C., "Finite-amplitude Instability or Parallel Shear Flows". <u>J. Fluid Mech.</u> (3), 27 (1967).
- Rosenbrook, G., "Instabilitat der Gleitschichten im schwach divergenten Kanal". ZAMM 17, 8 (1937).

- Schlichting, H., "Zur Entstehung der Turbulenz bei der Plattenstromung". Nachr. Ges. Wiss. Gott., Math. Phys. Klasse, (1933). Also, ZAMM, 13 (1933).
- Schubauer, G. B. and Klebanoff, P. S., "Contributions on the Mechanics of Boundary Layer Transition". NACA TN 3489 (1955) and NACA Rep. No. 1289 (1956).
- Schubauer, G. B. and Skramstad, H. K., "Laminar Boundary Layer Oscillations and Transition on a Flat Plate".

 National Bureau of Standards Research Paper 1772.

 Also, "Laminar Boundary Layer Oscillations and Stability of Laminar Flow". J. Aero. Sci., 14 (1947).
- Shen, S. F., "Calculated Amplified Oscillations in the Plane Poiseuille and Blasius Flows". J. Aero. Sci., 21 (1954).
- Sommerfeld, A., "Ein Beitrag Zur Hydrodynamischen Erklaerung Der Turbulenten Fluessigkeitsbewegungen". Atti del Congr. Internat. dei Mat., Rome (1908).
- Squire, H. B., "On the Stability for Three-Dimensional Disturbance of Viscous Fluid Flow between Parallel Walls". Proc. Roy. Soc. London, A 142, (1933).
- Stuart, J. T., "On the Stability of Viscous Flow Between Parallel Planes in the Presence of a Co-Planar Magnetic Field". Proc. Roy. Soc. A, 221 (1954).
- Stuart, J. T., "On the Effects of the Reynolds Stress on Hydrodynamic Stability". ZAMM Sonderheft (Special issue) 32-38 (1956). See also, J. Fluid Mech., 4 (1958) and J. Fluid Mech., 9 (1960).
- Thomas, L. H., "The Stability of Plane Poiseuille Flow".

 Physical Review (4), 91 (1953).
- Thompson, N. B., "Thermal Convection in a Magnetic Field".

 Phil. Mag. Ser. 7, 42 (1951).
- Tietjens, O., "Beitrage zur Entstenhung der Turbulenz". ZAMM, 5 (1925).
- Tollmein, W., "The Production of Turbulence". NACA Tech. Memo 609 (1931), originally published in Nachr. Ges. Wiss. Gott., Math. Phys. Klasse (1929).
- Tollmein, W., "General Instability Criterion of Laminar Velocity Distributions". NACA Tech. Memo 792 (1936), originally published in German in (1935).

ILLUSTRATIONS

(Tables and Figures)

Table 1. Comparison of Critical Eigenvalues

M		Lock		Presen	t Study	
	^α crit	Rcrit	P =	= 10 ⁻⁶	P _m	= 10 ⁻¹
			<u>α</u>	R	α	R
0	1.03	4000.	1.02	3847.	-	-
1	0.98	6960.	0.97	6782.	1.00	6926.
2	0.93	20000.	0.925	20160.	0.90	21180.
3	0.96	46000.	0.95	48230.	0.95	54600.
4	1.04	79400.	1.04	86340.	1.00	105100.
5	1.15	116700.	1.20	132300.	1.10	169400.
6	-	-	1.30	169500.	1.20	230700.

Note: Lock's original data has been converted to correspond to the same non-dimensional variables as used in this study, that is, R based on average velocity rather than centerline velocity.

Table 2. Eigenvalues for the Stability Equations for the Case of Neutral Stability ($c_i = 0.0$) M = 0.001, $P_m = 10^{-6}$

_α	R	c _r	Remarks
0.9780	26050.	0.2750	Upper Branch
1.0710	10050.	0.3400	
1.0980	5772.	0.3800	
1.0500	3924.	0.3997	
1.0200	3847.	0.3960	Critical Point
0.9500	4138.	0.3783	
0.8500	5426.	0.3417	
0.7500	8305.	0.2975	
0.6500	14620.	0.2500	
0.5756	26190.	0.2100	Lower Branch

Table 3. Eigenvalues for the Stability Equations for the Case of Neutral Stability ($c_i = 0.0$) M = 1.0, $P_m = 10^{-6}$

_α	R	c r	Remarks
1.0190	19580.	0.2900	Upper Branch
1.0480	10530.	0.3300	
1.0340	7866.	0.3470	
1.0000	6920.	0.3506	
0.9700	6782.	0.3474	Critical Point
0.9500	6853.	0.3436	
0.9000	7365.	0.3310	
0.8500	8388.	0.3148	
0.7500	12320.	0.2757	
0.6700	19250.	0.2400	Lower Branch

Table 4. Eigenvalues for the Stability Equations for the Case of Neutral Stability ($c_i = 0.0$) M = 1.0, $P_m = 10^{-1}$

<u> </u>	R	c r	Remarks
1.0330	15910.	0.3040	Upper Branch
1.0300	7641.	0.3490	
1.0000	6926.	0.3510	Critical Point
0.9000	7369.	0.3310	
0.8500	8388.	0.3152	
0.7500	12410.	0.2760	
0.6500	21920.	0.2311	Lower Branch

Table 5. Eigenvalues for the Stability Equations for the Case of Neutral Stability ($c_i = 0.0$) M = 2.0, $P_m = 10^{-6}$

α	R	c _r	Remarks
1.0070	40070.	0.2440	Upper Branch
0.9900	22830	0.2719	
0.9500	20380.	0.2741	
0.9250	20160.	0.2720	Critical Point
0.9000	20440.	0.2685	
0.8000	25630.	0.2446	
0.6500	53040.	0.1931	Lower Branch

Table 6. Eigenvalues for the Stability Equations for the Case of Neutral Stability ($c_i = 0.0$) M = 2.0, $P_m = 10^{-1}$

<u>α</u>	R	c r	Remarks
0.9726	66050.	0.2200	Upper Branch
0.9986	40240.	0.2450	
0.9900	25510.	0.2676	
0.9500	21430.	0.2730	
0.9000	21180.	0.2679	Critical Point
0.8500	22870.	0.2579	
0.7500	31716.	0.2291	
0.6500	53850.	0.1932	Lower Branch

Table 7. Eigenvalues for the Stability Equations for the Case of Neutral Stability ($c_i = 0.0$) M = 3.0, $P_m = 10^{-6}$

_α	R	c _r	Remarks
1.0380	134200.	0.1880	Upper Branch
1.0560	74400.	0.2140	
1.0300	54770.	0.2267	
1.0000	49650.	0.2294	
0.9500	48230.	0.2271	Critical Point
0.8600	54680.	0.2138	
0.7500	79570.	0.1878	
0.6500	136500.	0.1584	Lower Branch

Table 8. Eigenvalues for the Stability Equations for the Case of Neutral Stability ($c_i = 0.0$) M = 3.0, $P_m = 10^{-1}$

α	R	c r	Remarks
1.0140	143400.	0.1870	Upper Branch
1.0280	105600.	0.2000	
1.0170	66980.	0.2190	
0.9900	57850.	0.2238	
0.9500	54600.	0.2235	Critical Point
0.9000	55550.	0.2185	
0.8500	60540.	0.2102	
0.7500	84930.	0.1867	
0.6500	143900.	0.1577	Lower Branch

Table 9. Eigenvalues for the Stability Equations for the Case of Neutral Stability ($c_i = 0.0$) M = 4.0, $P_m = 10^{-6}$

α	R	c _r	Remarks
1.1570	178500.	0.1800	Upper Branch
1.1490	117900.	0.1970	
1.0900	88910.	0.2069	
1.0400	86340.	0.2057	Critical Point
0.9500	93620.	0.1969	
0.9000	104100.	0.1892	
0.8000	143800.	0.1697	Lower Branch

Table 10. Eigenvalues for the Stability Equations for the Case of Neutral Stability (c_i = 0.0) M = 4.0, $P_m = 10^{-1}$

α	R	c r	Remarks
1.1120	186000.	0.1800	Upper Branch
1.0900	132200.	0.1930	
1.0400	108000.	0.1986	
1.0000	105100.	0.1975	Critical Point
0.9500	108900.	0.1930	
0.9000	119000.	0.1865	
0.8000	159700.	0.1676	Lower Branch

Table 11. Eigenvalues for the Stability Equations for the Case of Neutral Stability ($c_i = 0.0$) M = 5.0, $P_m = 10^{-6}$

<u> </u>	R	c r	Remarks
1.2980	188100.	0.1820	Upper Branch
1.2540	148900.	0.1910	
1.2400	141400.	0.1928	
1.2300	140800.	0.1926	
1.2000	132300.	0.1945	
1.1500	127400	0.1944	Critical Point
1.1000	131000.	0.1912	
1.0000	148900.	0.1813	
0.9000	190200.	0.1666	Lower Branch

Table 12. Eigenvalues for the Stability Equations for the Case of Neutral Stability ($c_i = 0.0$) M = 5.0, $P_m = 10^{-1}$

<u>α</u>	R	c r	Remarks
1.1900	195700.	0.1810	Upper Branch
1.1700	184700.	0.1827	
1.1500	175400.	0.1840	
1.1000	169400.	0.1834	Critical Point
1.0500	175000.	0.1799	
1.0300	174600.	0.1789	
0.9820	186600.	0.1740	Lower Branch
			·

Table 13. Eigenvalues for the Stability Equations for the Case of Neutral Stability ($c_i = 0.0$) M = 6.0, $P_m = 10^{-6}$

_α	R	c _r	Remarks
1.466	199030.	0.1840	Upper Branch
1.378	176800.	0.1880	
1.350	171700.	0.1885	
1.300	169500.	0.1881	Critical Point
1.250	171300.	0.1865	
1.200	172800.	0.1844	
1.150	179300.	0.1813	
1.100	196400.	0.1758	
1.050	216000.	0.1701	Lower Branch
			·

Table 14. Eigenvalues for the Stability Equations for the Case of Neutral Stability (c $_{i}$ = 0.0) M = 6.0, P_{m} = 10^{-2}

α	R	c r	Remarks
1.450	211000.	0.1810	Upper Branch
1.380	185700.	0.1855	
1.300	175800.	0.1863	Critical Point
1.250	179200.	0.1843	
1.150	188400.	0.1791	
1.100	199700.	0.1752	
1.050	220600.	0.1692	Lower Branch

Table 15. Eigenvalues for the Stability Equations for the Case of Neutral Stability ($c_i = 0.0$) M = 6.0, $P_m = 10^{-1}$

<u>α</u>	R	c _r	Remarks
1.280	237400.	0.1765	Upper Branch
1.250	230800.	0.1771	
1.200	230700.	0.1756	Critical Point
1.150	234500.	0.1734	
1.111	245000.	0.1700	Lower Branch

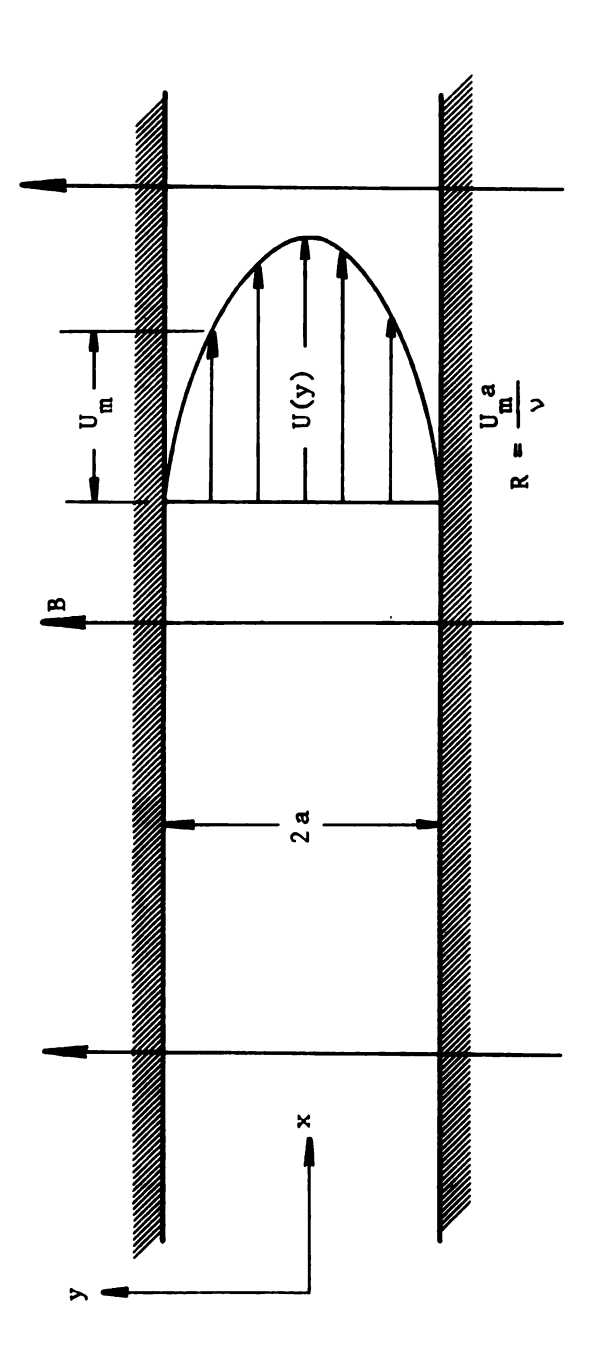


Figure 1. Primary Flow Configuration

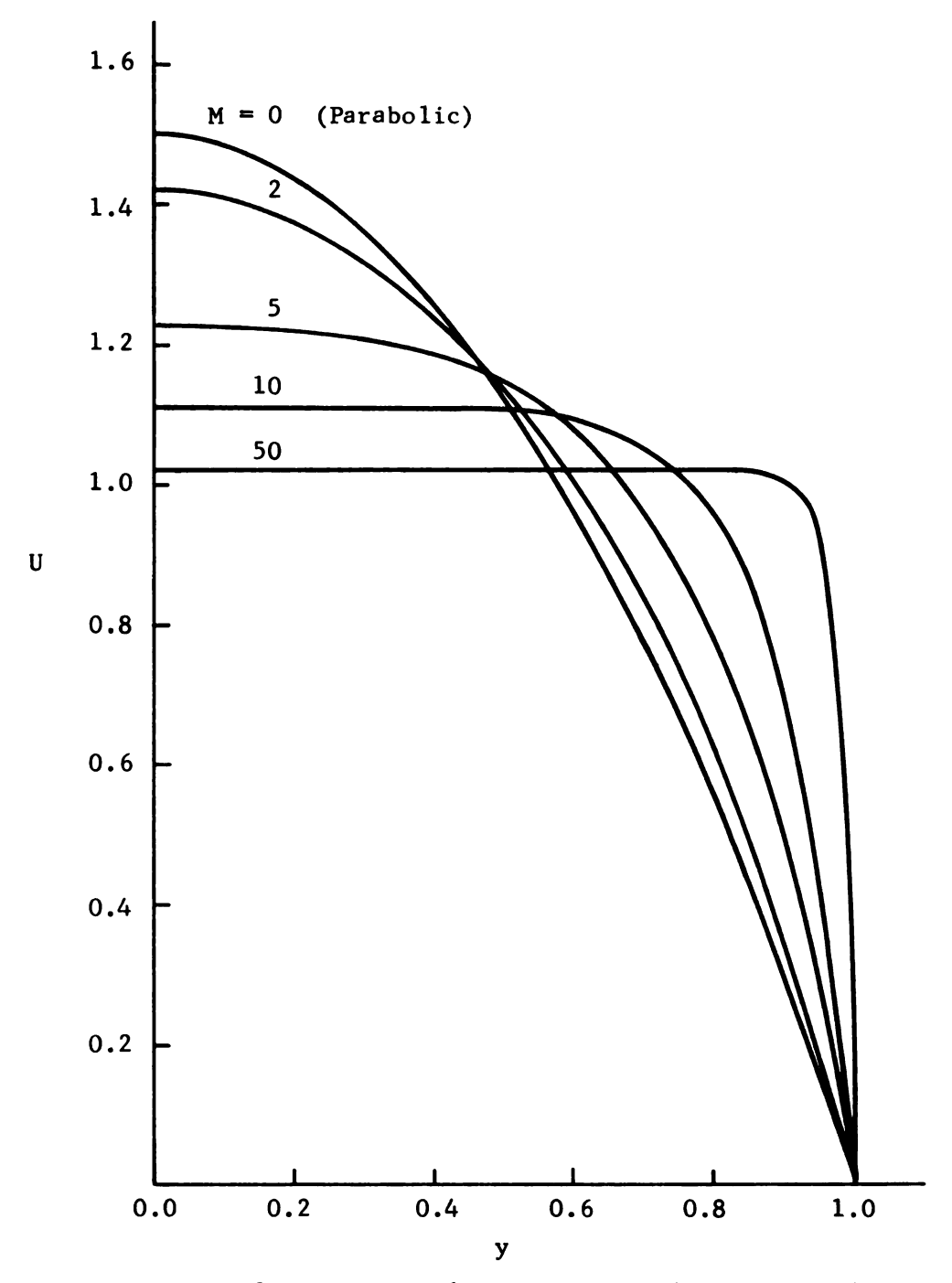


Figure 2. Dimensionless Primary Velocity Profiles for Various Hartmann Numbers

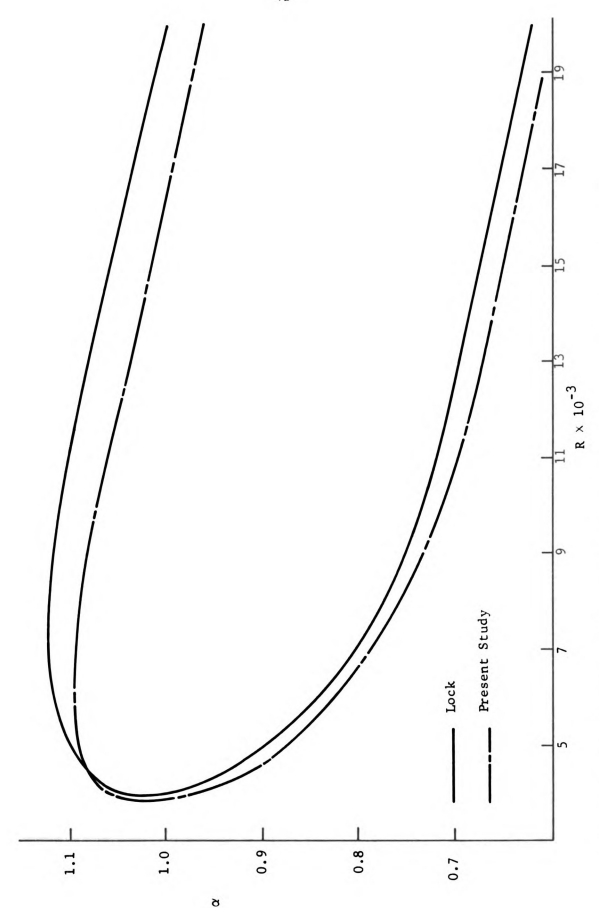


Figure 3. Wave Number α Versus Reynolds Number R for Neutral Stability for M = 0

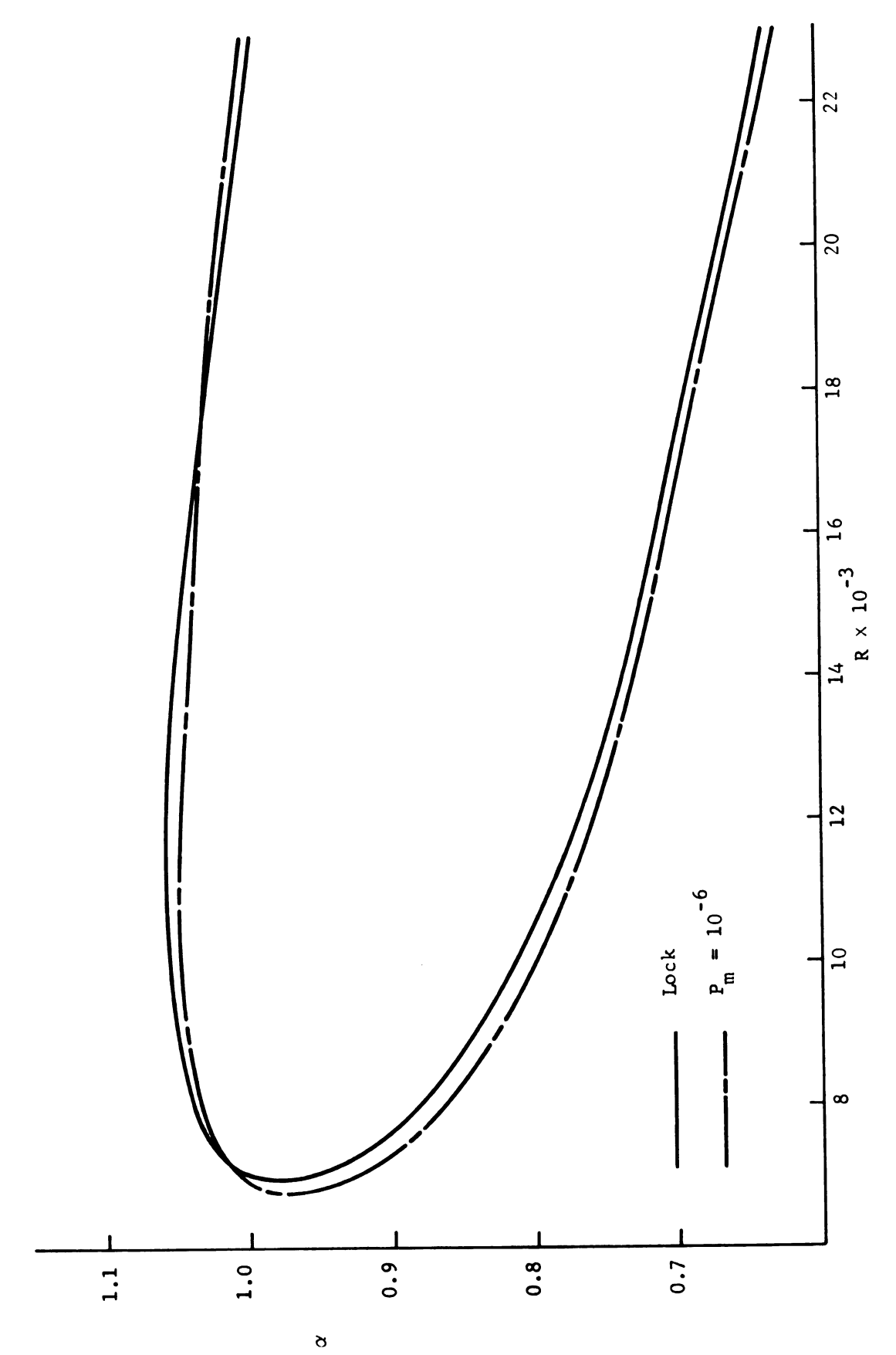
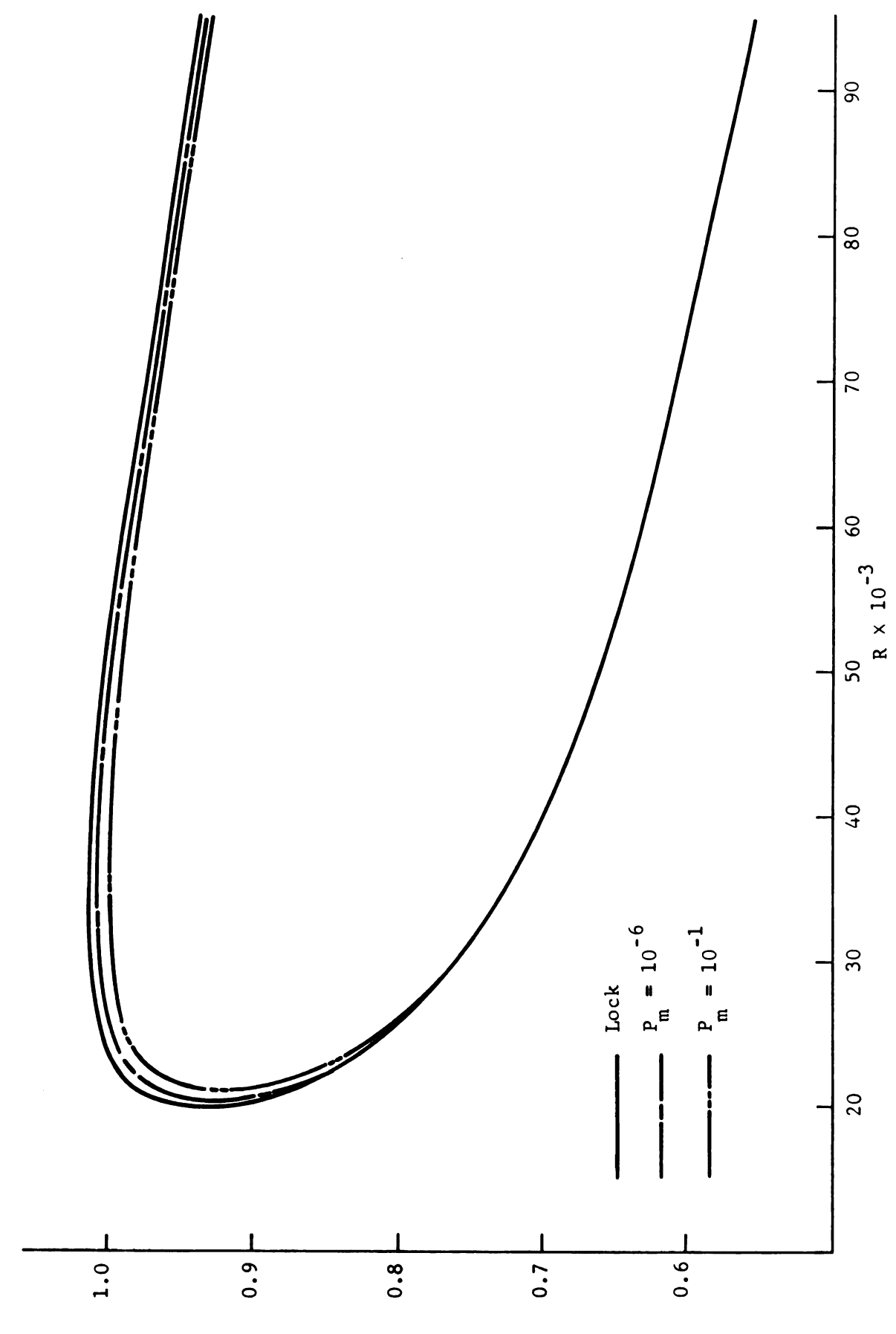
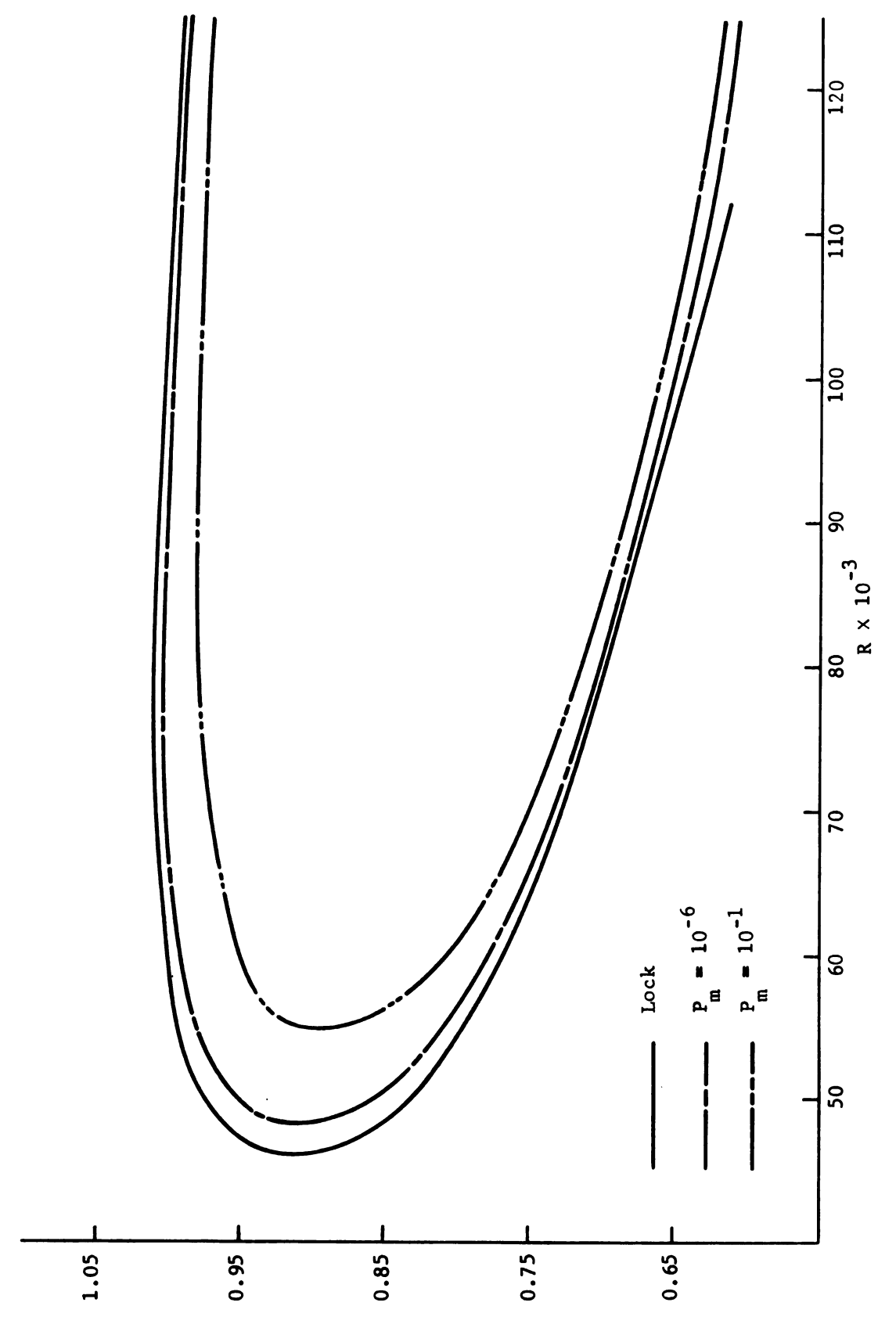


Figure 4. Wave Number a Versus Reynolds Number R for Neutral Stability for M = 1.0



b

Figure 5. Wave Number α Versus Reynolds Number R for Neutral Stability for M = 2.0



В

Figure 6. Wave Number α Versus Reynolds Number R for Neutral Stability for M = 3.0

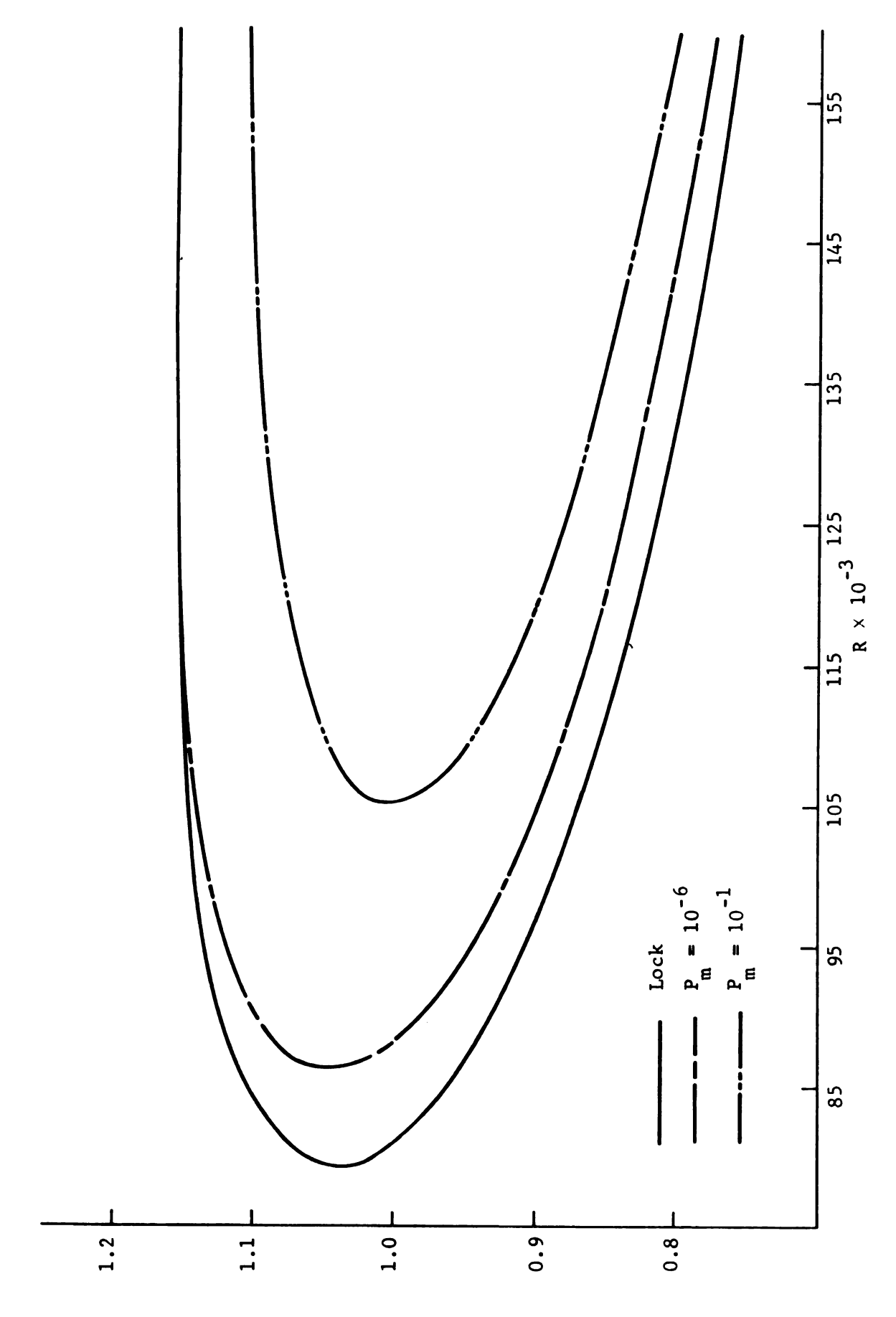


Figure 7. Wave Number α Versus Reynolds Number R for Neutral Stability for M = 4.0

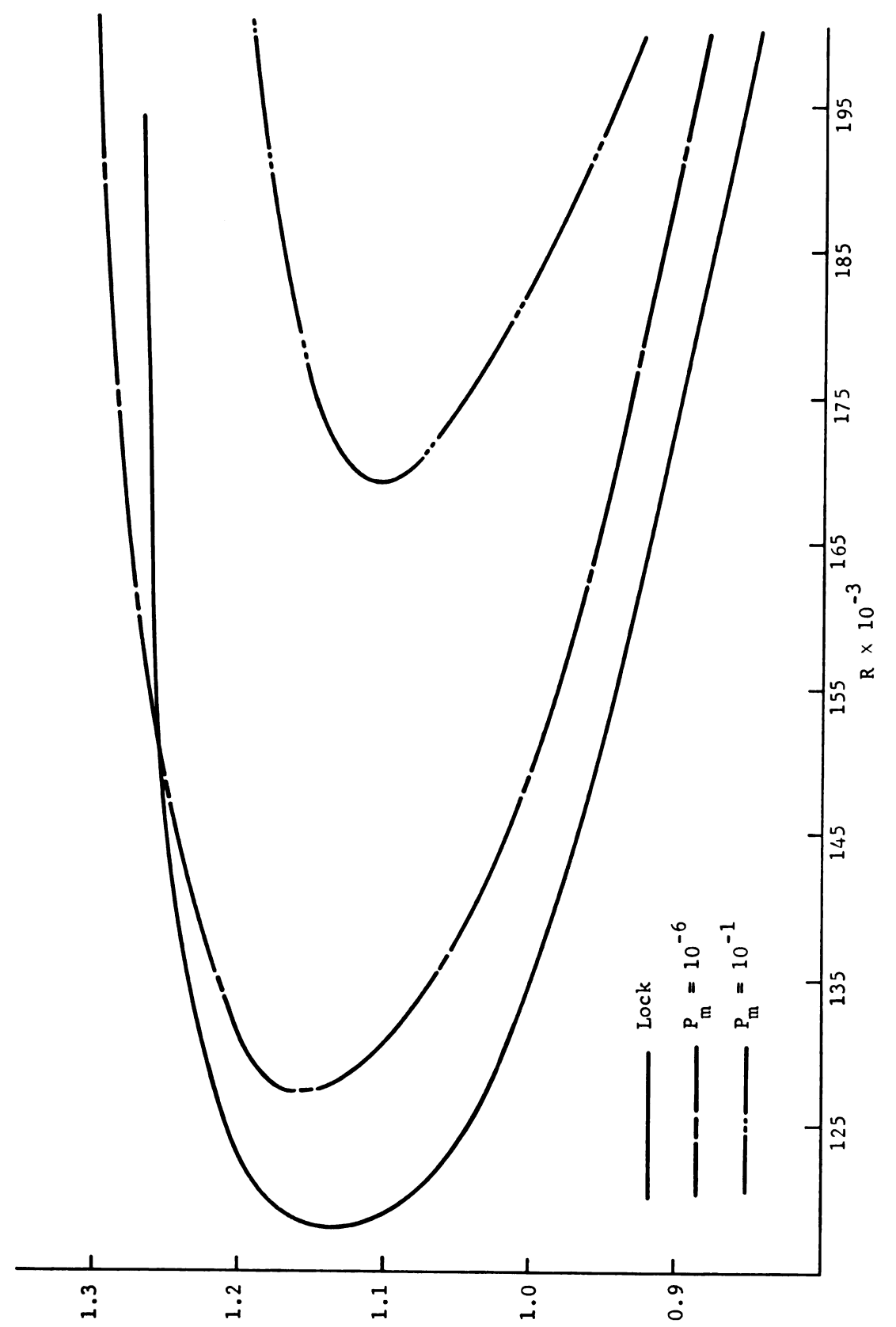
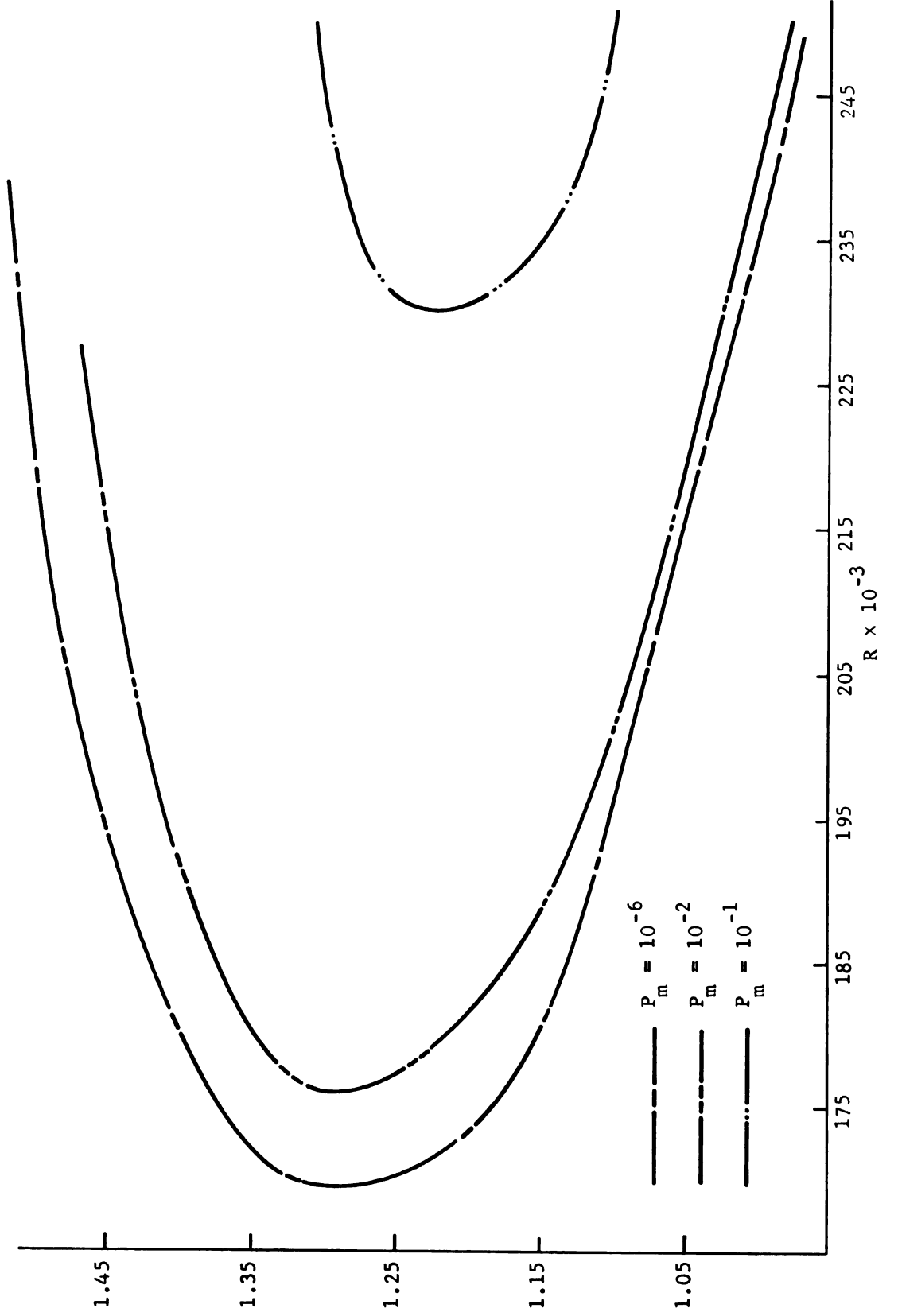
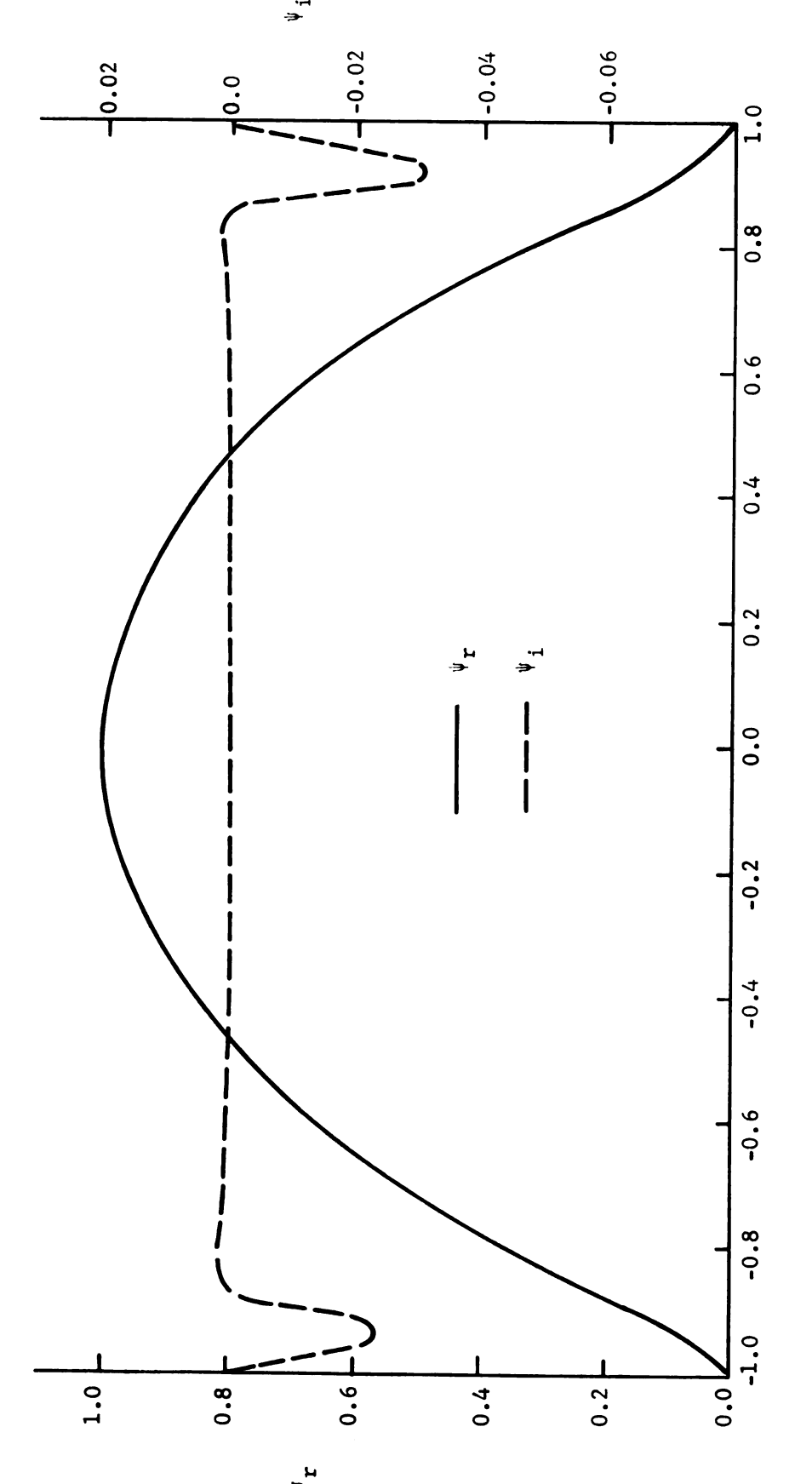


Figure 8. Wave Number α Versus Reynolds Number R for Neutral Stability for M = 5.0

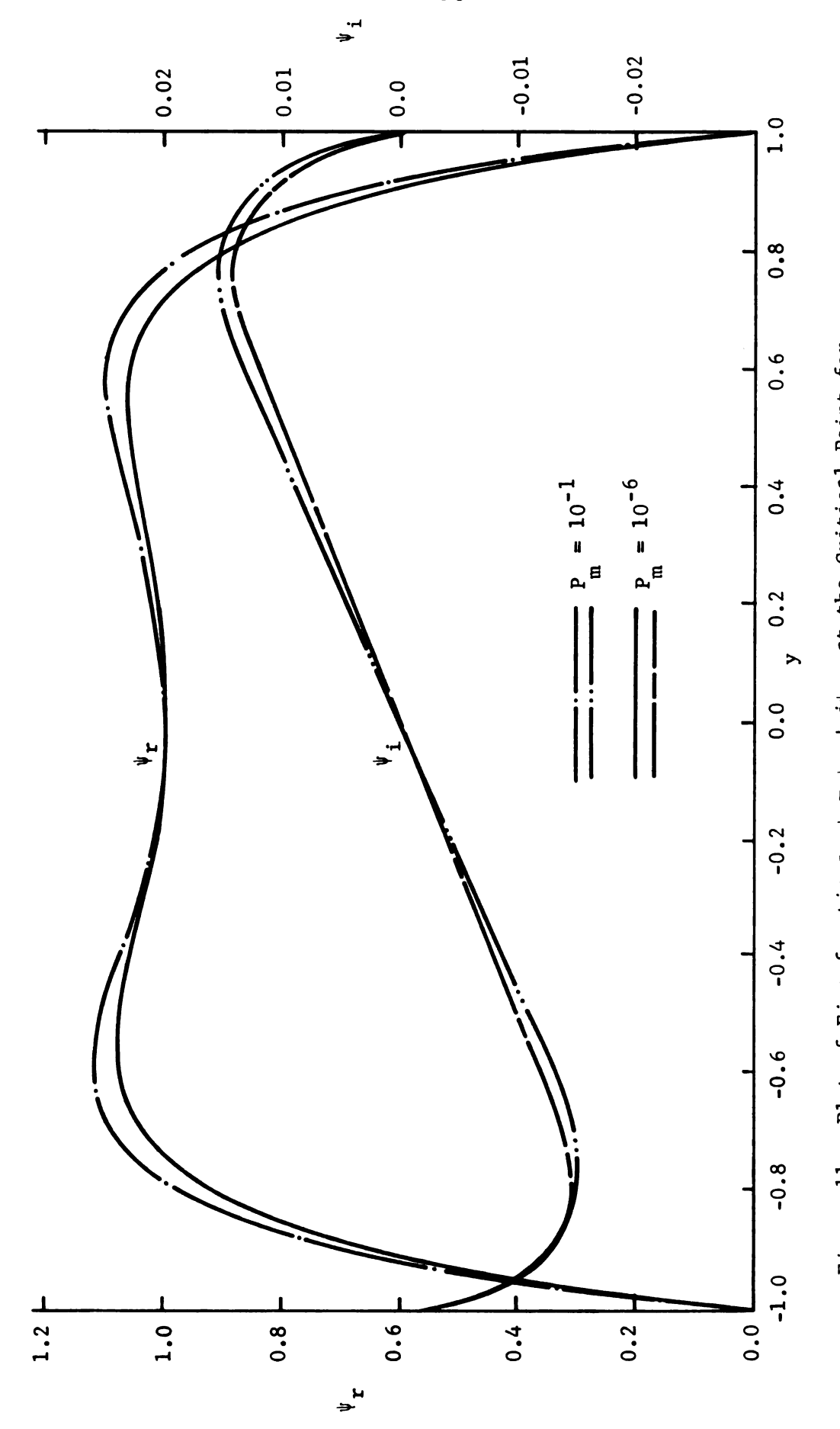


В

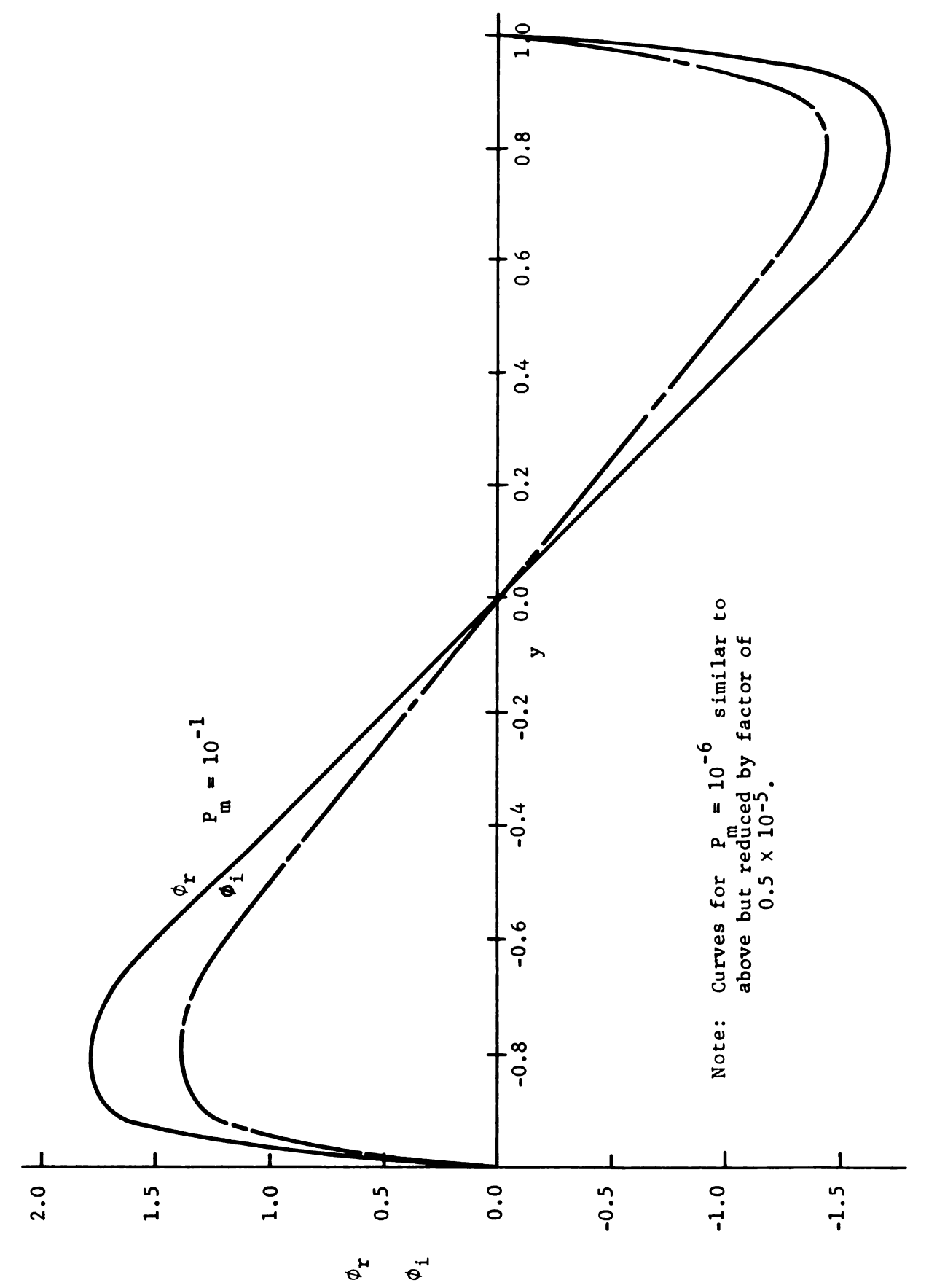
Figure 9. Wave Number lpha Versus Reynolds Number R for Neutral Stability for M = 6.0



at the Critical Point for M = 0.001Figure 10. Plot of Eigenfunctions $\psi = \psi_{\mathbf{r}} + i\psi_{\mathbf{i}}$



+ $i\psi_{\mathbf{i}}$ at the Critical Point for for M = 5.0Figure 11. Plot of Eigenfunctions $\psi = \psi_1$ $p = 10^{-6}$ and 10^{-1} for M in



at the Critical Point for Plot of Eigenfunctions $\phi = \phi + i\phi_i$ P = 10-6 and 10-1 for M $\stackrel{\square}{=}$ 5.0 Figure 12.

APPENDICES

APPENDIX A

Numerical Technique to Solve the Governing Stability Equations

A standard fourth order Runge-Kutta integration scheme was chosen in preference to a predictor-corrector scheme to simultaneously integrate the coupled second order and fourth order equations. The predictor-corrector scheme calculates the value of the highest order derivative based on a curve passed through the values at the previous three steps. All lower order derivatives are then calculated from this. Because of the large growth found to exist for some of the eigenfunctions and the suppression scheme used, variations in the highest order derivative (in particular, the fourth derivative) caused significant changes in the final eigenvalues. The Runge-Kutta method is not subject to this since each derivative is essentially calculated separately at each step. In fact, the fourth derivative at each step need not be calculated, so to save time and machine storage this derivative was eliminated from the computer program.

The accuracy of the results were verified by running the non-magnetic plane Poiseuille case and comparing the results against Thomas (1958) and Reynolds and Potter (1967). Rather than write a separate program for the single fourth order equation the present program was run for a Hartmann number of 10^{-3} . This was effectively zero and gave excellent results, which agreed to three significant figures to the presently accepted

values.

Several runs were made for various step sizes, with 0.01 chosen as the optimum. Doubling this value resulted in eigenvalues that were in error by about four percent, while halving this value resulted in a change in eigenvalues of only 0.4%. Based upon these results, a step size of 0.01 provided accurate values without excessive computation time or machine storage requirements. For this step size, the truncation error associated with the Runge-Kutta scheme is of the order of 10^{-10} .

The scheme as illustrated by Collatz (1951) is outlined below:

At
$$y$$

$$v_{00} = \psi(y)$$

$$v_{10} = \Delta \psi'(y)$$

$$v_{20} = \frac{\Delta^2}{2} \psi''(y)$$

$$v_{30} = \frac{\Delta}{6} \psi''''(y)$$

$$v_{00} = \phi(y)$$

$$v_{10} = \Delta \phi'(y)$$

Using equations (2.4.8) and (2.4.9)

$$\begin{aligned} \mathbf{F}_{1} &= \frac{\Delta^{2}}{2} \ \mathbf{f}(\frac{\mathbf{v}_{10}}{\Delta}, \ \mathbf{v}_{00}, \ \mathbf{u}_{00}, \ \mathbf{y}) \\ &= \frac{\Delta^{2}}{2} \ \{ \left[\mathbf{i} \ \alpha \ \mathbf{R}_{\mathbf{m}}(\mathbf{U} - \mathbf{c}) \ + \ \mathbf{K}^{2} \right] \phi^{\dagger} \ - \ \mathbf{i} \ \alpha \ \mathbf{R}_{\mathbf{m}}^{\mathbf{h}\psi} \ - \ \mathbf{R}_{\mathbf{m}}^{\psi} \, \} \end{aligned}$$

$$G_{1} = \frac{\Delta^{4}}{24} f(\frac{2V_{20}}{\Delta^{2}}, \frac{V_{10}}{\Delta}, V_{00}, \frac{U_{10}}{\Delta}, U_{00}, y)$$

$$= \frac{\Delta^{4}}{24} \{ [i \alpha R(U-c) + 2K^{2} + M^{2}]\psi'' + 2 i \alpha M^{2}H \psi'$$

$$- [i \alpha R K^{2}(U-c) + i \alpha R U'' + K^{4} + \alpha^{2}M^{2}h^{2} - i \alpha M^{2}h']\psi$$

$$- i \alpha M^{2}(U-c)\phi' + [\alpha^{2}M^{2}h(U-c) - i \alpha M^{2}(U'-h''/R_{m})]\phi \}$$

where $\Delta = \Delta Y = \text{step size}$

Values at
$$Y + \frac{\Delta Y}{2}$$

$$\begin{aligned} \mathbf{v}_{01} &= \mathbf{v}_{00} + \frac{1}{2} \, \mathbf{v}_{10} + \frac{1}{4} \, \mathbf{v}_{20} + \frac{1}{8} \, \mathbf{v}_{30} + \frac{1}{16} \, \mathbf{G}_{1} \\ \mathbf{v}_{11} &= \mathbf{v}_{10} + \mathbf{v}_{20} + \frac{3}{4} \, \mathbf{v}_{30} + \frac{1}{2} \, \mathbf{G}_{1} \\ \mathbf{v}_{21} &= \mathbf{v}_{20} + \frac{3}{2} \, \mathbf{v}_{30} + \frac{3}{2} \, \mathbf{G}_{1} \\ \mathbf{v}_{31} &= \mathbf{v}_{30} + 2 \, \mathbf{G}_{1} \\ \mathbf{v}_{01} &= \mathbf{v}_{00} + \frac{1}{2} \, \mathbf{v}_{10} + \frac{1}{4} \, \mathbf{F}_{1} \\ \mathbf{v}_{11} &= \mathbf{v}_{10} + \mathbf{F}_{1} \end{aligned}$$

As before

$$F_{2} = \frac{\Delta^{2}}{2} f(\frac{v_{11}}{\Delta}, v_{01}, u_{01}, y)$$

$$G_{2} = \frac{\Delta^{4}}{24} f(\frac{2v_{21}}{\Delta^{2}}, \frac{v_{11}}{\Delta}, v_{01}, \frac{u_{11}}{\Delta}, u_{01}, y)$$

Values at $Y + \Delta Y$

$$v_{02} = v_{00} + v_{10} + v_{20} + v_{30} + G_{2}$$

$$v_{12} = v_{10} + 2 v_{20} + 3 v_{30} + 4 G_{2}$$

$$v_{22} = v_{20} + 3 v_{30} + 6 G_{2}$$

$$v_{32} = v_{30} + 4 G_{2}$$

$$v_{02} = v_{00} + v_{10} + F_{2}$$

$$v_{12} = v_{10} + 2 F_{2}$$

Again as before

$$F_{3} = \frac{\Delta^{2}}{2} f(\frac{V_{12}}{c}, V_{02}, U_{02}, Y)$$

$$G_{3} = \frac{\Delta^{4}}{24} f(\frac{2V_{22}}{\Delta^{2}}, \frac{V_{12}}{\Delta}, V_{02}, \frac{U_{12}}{\Delta}, U_{02}, Y)$$
and
$$F = \frac{1}{3} (F_{1} + 2 F_{2})$$

$$F' = \frac{1}{3} (F_{1} + 4 F_{2} + F_{3})$$

$$G = \frac{1}{15} (8 G_{1} + 8 G_{2} - G_{3})$$

$$G' = \frac{1}{5} (9 G_{1} + 12 G_{2} - G_{3})$$

$$G''' = 2 (G_{1} + 2 G_{2})$$

$$G'''' = \frac{2}{3} (G_{1} + 4 G_{2} + G_{3})$$

Thus the functions and their derivatives at $Y + \Delta Y$ are

$$\psi(y + \Delta y) = V_{00} + V_{10} + V_{20} + V_{30} + G$$

$$\psi'(y + \Delta y) = \frac{1}{\Delta y} (V_{10} + 2 V_{20} + 3 V_{30} + G')$$

$$\psi''(y + \Delta y) = \frac{2}{(\Delta y)^2} (V_{20} + 3 V_{30} + G'')$$

$$\psi'''(y + \Delta y) = \frac{6}{(\Delta y)^3} (V_{30} + G''')$$
and
$$\phi(y + \Delta y) = U_{00} + U_{10} + F$$

$$\phi'(y + \Delta y) = \frac{1}{\Delta y} (U_{10} + F')$$

Now, if desired, $\psi''''(y+\Delta y)$ and $\phi''(y+\Delta y)$ can be calculated from the above.

Implementing the formulas in the sequence given, the integration is started at one wall and proceeds across the channel to the other wall where the combined functions are formed.

APPENDIX B

COMPUTER PROGRAM

B-1 Description of the Computer Program

The program initially reads the required values for loop sizes, internal program counters, step size, convergence criteria, the initial guesses for the eigenvalues, and also sets boundary conditions at the wall.

Subroutine RUNGE is now called which in turn calls

Subroutine VCAl to calculate the value of the mean velocity

and induced magnetic field and their derivatives which are

known inputs to Runge. The equations are now integrated to

determine the value of the function and its derivatives at the

next step.

Returning to the main program, the number one solution which is the growing solution is filtered from solutions two and three. To further insure independency, solution number two is filtered from number three.

The above procedure is repeated until the filtered solutions are obtained across the entire channel.

At the next stage the filtered solutions are corrected to account for the portion filtered out and then printed out if this option has been selected. Next the growing solution is modified to compress the magnitude range of the functions.

The three independent solutions are now combined linearly to find the total function and the derivatives at the opposite wall. A test function based on ψ_w is checked to see if the boundary condition namely $\psi_w = 0$, is satisfied. If not, the eigenvalues are each incremented by a small amount and a new guess is made for the eigenvalues. The process is repeated until convergence is achieved or the iteration counter exceeds its present value.

The program incorporates a printout monitor which allows the selection of 3 levels of printout. The value of the monitor is read in and can be assigned values from one to three. A value of one provides express runs and gives the eigenvalues and values of the test function at the end of each iteration; two prints out the above plus the final combined eigenfunctions; and a value of three prints out all the eigenfunctions. When using the two or three option an additional parameter is read in that specifies the number of increments between printout points.

Explanation of the Input Cards for the Main Program

Card Number	Column	<u>Item</u>	Format	Program Designation
1	1-10	Printout monitor	I 10	NCM
	11-20	No. of data cards	I 10	KP
	21-30	Max. No. of iterations	I 10	IT
	31-40	Steps between printout pts.	I 10	IJ
	41-50	Step size	F 10.5	DELY
2	1-10	Percent change in c	F 10.5	PAL
	11-20	Percent change in R	F 10.5	PCR
	21-30	Maximum change in c or R	F 10.5	PCH
	31-40	Convergence criteria	E 10.5	TIP

Card <u>Number</u>	Co lumn	Item	Format	Program Designation
3	1-10	A 1 pha	F 10.5	AL
	11-20	Reynolds number	F 10.5	R
	21-30	c _r	F 10.5	CR
	31-40	c i	F 10.5	CI
	41-50	Beta	F 10.5	BE
	51-60	Hartmann No.	F 10.5	нм
	61-70	Magnetic Prandtl No.	E 10.3	PM

Any number of data cards as shown by card number 3 above may be added.

B-2 Listing of the Computer Program

The program developed to compute the eigenvalues for any given case is listed in the next section. Actually two versions of this program were used to obtain the data points used in plotting the curves presented. They differed only in regard to which of the eigenvalues was held fixed while iterating on the other two. The program listed here is called MHDA which holds α constant and iterates on c_r and R. This program was used on the lower leg of the stability curve up to and slightly beyond the critical point. Since the upper leg of the curve is relatively flat the second version was used which fixed c_r and iterated on α and R. This procedure minimized the number of "bad guesses" which result in no convergence and also to conserve computer time by more evenly distributing the points along the curve.

The programs were run on the CDC 6500 and took a little over 4 seconds per pass (one third of an iteration) with convergence obtained in normally three to four iterations.

In the program that follows, the dollar sign statement separator and multiple replacement statements are used to reduce the size of the source deck.

```
PROGRAM MHDA(INPUT, OUTPUT, TAPE2=INPUT, TAPE3=OUTPUT)
         THIS PROGRAM ITERATES ON CR AND REY NO WITH ALPHA CUNSTANT
      DIMENSIUN RR(201,3),Z(201),Q(3),G(3),RS(3),A(3,3),B(3,3),W(3),
     1X(3).T(3).TEST(3)
      COMMON P(201,3), DP(201,3), DPP(201,3), D3P(201,3), V(201,3), DV(201,3)
     1,C1,C2,C3,C4,U0(3),AL,RE,CW,R,DELY,C,K,XM
      COMPLEX P.DP.D2P.D3P.V.DV.U1.U2.U0.RR.RS.A.B.B1.B2.B3.T.Q.X.
     1W,DT1,DT2,CW,A1,A2,A3,A4,A5,A6,A7,A8,C1,C2,C3,C4
C
         READ IN PROGRAM PARAMETERS AND INITIAL GUESSES
      READ(2,400) MON, KP, IT, JJ, DFLY
      READ(2,401) PAL, PCR, PCH, TIP
      N=2.0001/DFLY+1 $ NM=N-1 $ KK=0 $ C=DELY
  100 KK=KK+1 $ IP=MD=KL=0 $ ITF=1
      IF(KK-KP) 600,600,250
  600 CONTINUE
      KEAF (2,402) AL,R,CW,BE,HM,PM
      CF=REAL(CW) & CI=AIMAG(CW) & XM=HM#HM
      WRITF (3,819) HM, PM, CI, BE, DELY
  101 MD=ME+1
      IF(IP-0) 598,598,599
  598 KRITE(3,801) ITE
  599 IF(MD-IT) 602,602,601
  601 WRITE(3,803) $ 60 TO 100
  602 WRITE (3,802) R,AL,CR
      K=AL*AL+BF*HF $ Y=-1.0 $ 2(1)=-1.0 $ KM=PM*K
      CW=CR
         BO INDARY CONDITIONS ---- PEDPEVEO AT Y=+-1
(
         V=PHI=MAGNETIC PERTURBATIONS, P=PSI=VFLUCITY PERTURBATIONS
         SET STARTING CONDITIONS
      P(1,1)=P(1,2)=P(1,3)=0P(1,1)=0P(1,2)=0P(1,3)=(0.0,0.0)
      V(1,1)=V(1,2)=V(1,3)=(0.0,0.0)
      PV(1,1)=(1.1-130,1.1-130) $ PV(1,2)=PV(1,3)=(0.0,0.0)
      DP(1,3)=(1.0,1.0) $ DP(1,1)=DP(1.2)=(0.0,0.0)
      0.3P(1,2)=(1.0,1.0) $ 0.3P(1,1)=0.3P(1,3)=(0.0,0.0)
      Cl=(0.0.1.0) $ C2=C1*AL*RM $ C3=C1*AL*R $ C4=C1*AL*XM
      DO 300 J=1,NM & LL=J
         GENERATE 3 SOLUTIONS AT EACH STEP
      CALL RUNGFILL, Y, HM, RM)
      L= J+1 & Z(L)=Z(J)+DELY
         EXTRACT THE GROWING SOLUTION (NO.1) FROM SULNS 2 AND 3
      UU=ABS(FEAL(UO(1)))
      IF (IIII-1.F125) 178,179,179
  179 00(1)=00(1)*(1.4-100)
  179 00 299 1=2.3
      IF (UU-1.E125) 171,172,172
  171 PR(L,1)=U0(1)/U0(1)
      GO TO 173
  172 RR(L,1)=(00(1)/00(1))*(1.F-100)
        P(L,1) = P(L,1) - RP(L,1) * P(L,1)
       UP(L,I) = DP(L,I) - RR(L,I) + DP(L,I)
      0.2P(L,I)=0.2P(L,I)-RR(L,I)*0.2P(L,I)
```

```
D3P(L,I)=D3P(L,I)-RR(L,I)*D3P(L,I)
        V(L,I)=V(L,I)-RR(L,I)+V(L,I)
       DV(L,I) = DV(L,I) - RR(L,I) + DV(L,I)
  299 CONTINUE
C
         EXTRACT SOLUTION 2 FROM 3
      RR(L,1)=U0(3)/U0(2)
      P(L,3)=P(L,3)-RR(L,1)+P(L,2) $ DP(L,3)=DP(L,3)-RR(L,1)+DP(L,2)
      D2P(L,3)=D2P(L,3)-RR(L,1)*D2P(L,2)
      D3P(L,3)=D3P(L,3)-RR(L,1)+D3P(L,2)
      V(L,3)=V(L,3)-RR(L,1)+V(L,2) $ DV(L,3)=DV(L,3)-RR(L,1)+DV(L,2)
  300 CONTINUE
C
         REPAIR THE EXTRACTIONS
      IF(MON-1) 508,508,632
  632 J=N $ NN=N-2 $ RS(2)=RR(J,2) $ RS(3)=RR(J,3)
      DO 303 MM=1,NN $ J=J-1 $ DO 303 I=2,3
      P(J,I)=P(J,I)-RS(I)+P(J,I) $ D3P(J,I)=D3P(J,I)-RS(I)+D3P(J,I)
      DP(J,I)=DP(J,I)-RS(I)*DP(J,I) $ D2P(J,I)=D2P(J,I)-RS(I)*D2P(J,I)
      V(J,I)=V(J,I)-RS(I)+V(J,I) $ DV(J,I)=DV(J,I)-RS(I)+DV(J,I)
  303 RS(1)=RS(1)+RF(J,1)
      J=N SRS(1)=RR(J,1) SI=3
      DO 631 MM=1,NN S J=J-1
      P(J,I)=P(J,I)-RS(1)+P(J,2) $ D3P(J,I)=D3P(J,I)-RS(1)+D3P(J,2)
      DP(J,I)=DP(J,I)-RS(1)+DP(J,2) + D2P(J,I)=D2P(J,I)-RS(1)+D2P(J,2)
      V(J,I)=V(J,I)-RS(I)*V(J,2) $ DV(J,I)=DV(J,I)-RS(I)*DV(J,2)
  631 RS(1)=RS(1)+RR(J,1)
C
         PRINT OUT THE INDEPENDENT EIGENFUNCTIONS IF DESIRED
      GO TO (508,508,507), MON
  507 WPITF(3,807) $ DO 319 I=1,3 $ WRITE(3,805) I $ DO 311 J=1,N,JJ
  311 WRITE(3,806) Z(J),P(J,1),OP(J,1),O2P(J,1),O3P(J,1)
      WRITF(3,816) $ DO 344 J=1,N,JJ
  344 WRITE(3,806) Z(J),V(J,1),DV(J,1)
  319 CONTINUE
  508 CONTINUE $ NC=N/2+1 $ J=N
         MODIFY THE GROWING SOLUTION
      IF(UU-1.E125) 175,174,174
  174 AB=P(N,1)*(1.E-100) $ A5=P(N,2)/AB*(1.F-100) $ GU TO 176
  175 A5=P(N,2)/P(N,1)
  176 DO 307 KJ=1,NM
        P(J,1) = P(J,2) - A5 = P(J,1)  P(J,1) = P(J,2) - A5 = P(J,1)
      D2P(J,1)=D2P(J,2)-A5*D2P(J,1) $ D3P(J,1)=D3P(J,2)-A5*D3P(J,1)
      V(J,1)=V(J,2)-A5*V(J,1) $ DV(J,1)=DV(J,2)-A5*DV(J,1)
  307 J=J-1
      GO TO (506,506,505),MON
  505 WRITE(3,804) $ I=1 $ WRITE(3,805) I $ DO 310 J=1,N,JJ
  310 WRITE(3,806) Z(J),P(J,1),DP(J,1),D2P(J,1),D3P(J,1)
      WRITE(3,816) $ 00 345 J=1,N,JJ
  345 WRITE(3,806) Z(J),V(J,I),DV(J,I)
  506 CONTINUE
C
         DETERMINE THE TOTAL SOLUTION AT OPPOSITE WALL
      A(1,1)=V(N,1) $ A(1,2)=V(N,2) $ A(1,3)=V(N,3)
      A(2,1) = DP(N,1)    A(2,2) = DP(N,2)    A(2,3) = DP(N,3)
      A(3,1)=D2P(N,1) $ A(3,2)=D2P(N,2) $ A(3,3)=D2P(N,3)
```

```
B1=P(N,1) $ B2=P(N,2) $ B3=P(N,3)
         CALCULATE THE COEFFICIENTS NEEDED TO COMBINE THE FUNCTIONS
C
      C1=A(3,1)+(A(1,2)+A(2,3)-A(2,2)+A(1,3))-A(3,2)+(A(1,1)+A(2,3))
     1-A(2,1)+A(1,3))-A(3,3)+(A(1,2)+A(2,1)-A(1,1)+A(2,2))
      IF (UU-1.E125) 691,692,692
  692 C1=C1*(1.F-100)
  691 X(1) = -(A(2,2) + A(1,3) - A(1,2) + A(2,3))/C1
      X(2) = -(A(1,1) + A(2,3) - A(2,1) + A(1,3))/C1
      X(3) = -(A(1, 2) * A(2, 1) - A(1, 1) * A(2, 2))/C1
      1F(UU-1.E125) 693,694,694
  694 \times (1) = X(1) * (1.6-100)    X(2) = X(2) * (1.6-100)    X(3) = X(3) * (1.6-100)
         CHECK TOTAL SOLUTIONS AT THE WALL
C.
  693 W(1)=X(1) +A(1,1)+X(2)+A(1,2)+X(3)+A(1,3)
      W(2)=X(1)*A(2,1)+X(2)*A(2,2)+X(3)*A(2,3)
      W(3)=X(1)*A(3,1)+X(2)*A(3,2)+X(3)*A(3,3)-(1.0,0.0)
      WRT=0.0 $ DU 305 I=1.3
  305 WRT=WRT+ABS(REAL(W(I)))+ABS(AIMAG(W(I)))
      WRITE(3,811) WRT
      IF (WRT-1.F-10) 610,610,609
  609 WRITE(3,808) W(1), W(2), W(3) $ WRITE(3,813) $ GO TO 509
  610 IP=IP+1
         COMPUTE TEST FUNCTION
C
      T(IP)=X(1)*B1+X(2)*B2+X(3)*R3
      TEST(IP)=REAL(T(IP)*CONJG(T(IP)))
      IF(TEST(IP)-T1P) 611,611,612
  612 IF(KL-1) 614,613,613
  613 WRITE(3,812) T(IP), TEST(IP)
  614 WRITE(3,814) $ KL=0
         ITERATION OF EIGENVALUES
  525 GG TO (502,503,504),1P
  502 DCR=PAL +CR $ CR=CR+DCR $ GO T() 101
  503 CR=CR-DCR $ RD=PCR*R $ R=R+RD $ GU TO 101
  504 DT1=(T(2)-T(1))/DCR $ R=R-RD
      DT2=(T(3)-T()))/RD
      DEN=AIMAG((CONJG(DT1))*DT2)
      DCR = AIMAG(T(1) + CONJG(DT2))/DEN
      RD=AIMAG((CDNJG(T(1)))*DT1)/DEN
      IF (ABS(DCR).GE.(PCH*CR)) DCR=PCH*CR*CCR/ABS(DCR)
      IF(ABS(RU)-(PCH#R)) 616,616,615
  615 RD=PCH#R#RU/ABS(RD)
  616 R=R+R!) $ CR=CR+OCR $ 1P=0 $ 1TE=ITE+1 $ KL=1 $ GU TO 101
  611 WRITE(3,815) $ WRITE(3,8)2) T(1P),TEST(1P)
         PRINT OUT THE FINAL COMBINED FUNCTIONS IF DESIRED
  509 IF(MON-2) 100,511,511
  511 WRITE(3,809) $ WRITE(3,810) $ 00 315 J=1,N,JJ
      \Delta 1 = X(1) + P(J, 1) + X(2) + P(J, 2) + X(3) + P(J, 3)
      \Delta 2 = X(1) + OP(J, 1) + X(2) + DP(J, 2) + X(3) + DP(J, 3)
      A3=X(1)*D2P(J,1)+X(2)*D2P(J,2)+X(3)*D2P(J,3)
      A4=X(1)*D3P(J,1)+X(2)*D3P(J,2)+X(3)*D3P(J,3)
  315 WRITE(3,820) Z(J),A1,A2,A3,A4
      WRITE(3.821) $ 00 316 J=1.N.JJ
      A6=X(1)*V(J,1)+X(2)*V(J,2)+X(3)*V(J,3)
```

```
A7=X(1)+DV(J.1)+X(2)+DV(J.2)+X(3)+DV(J.3)
  316 WRITE(3.820) Z(J).A6.A7
  510 CONTINUE $ GO TO 100
  400 FORMAT(4110, F10.5)
  401 FORMAT(3F10.5,E10.5)
  402 FORMAT(6F10.5, E10.3)
  801 FORMAT(14HOITERATION NO.. 12)
  802 FORMAT(15HOREYNOLDS NO. =,F20.13,10X,7HALPHA =,F8.4,10X,
     14HCR = 1 F 20 - 141
  803 FORMAT(20HOEXCESSIVE ITERATION)
  804 FORMAT(27HOCORRECTED GROWING SOLUTION)
  80> FORMAT (14HOSOLUTION NO. ,12,/,1HO,3X,1HY,10X,6HP(J,1),18X,7HDP(J,
     11),16x,8HD2P(J,1),16x,8HD3P(J,1),16x,8HD4P(J,1))
  HO6 FORMAT(1H ,F5.2,5(E13.3,E12.3))
  807 FORMAT(24HOREPAIRED EIGENFUNCTIONS)
  808 FORMAT(1H0,3HVW=,E15.5,E15.5,/,7HODPS1W=,E15.5,E15.5,/,
     18HOD2PSIW=, E15.5, E15.5)
  809 FORMAT(25H1FINAL COMBINED FUNCTIONS)
  810 FURMAT(5x,1HY,12x,4HP(J),19x,5HDP(J),18x,6HD2P(J),18x,6HD3P(J),
     1 18X,6HD4P(J))
  811 FORMAT(27HOCUMULATIVE ERROR AT WALL =,E15.5)
  812 FORMAT(1H0,11HP AT WALL =,2E15.5,10x,15HTEST FUNCTION =,E15.5)
  813 FORMAT(30HOFUNCTIONS ON NOT SATISFY R.C.)
  814 FORMAT(//)
  815 FORMAT(27HOCONVERGENCE TEST SATISFIED)
  816 FORMAT(1H0,3X,1HY,10X,6HV(J,I),18X,7HDV(J,I),16X,8HD2V(J,I))
  819 FORMAT(26H) THE FOLLOWING CASE IS FOR, /, 14H HARTMANN NO. =, F7.3,
     15x,18HMAGNETIC PRANDTL =, E12.3,5x,4HCI =, F6.3,5x,6HBETA =, F6.3,
     2 /,12H STEP SIZE =,F6.3,///)
  820 FORMAT(1x, F5.2, 5(E12.3, E12.3))
  821 FORMAT(1H0,4X,1HY,12X,4HV(J),19X,5HDV(J),18X,6HD2V(J))
  250 CONTINUE
      END
      SUBROUTINE RUNGE (J.Y.HM.RM)
С
         THIS SUBROUTINE USES A FOURTH ORDER RUNGE-KUTTA SCHEME
      DIMENSION G(2)
      COMMON P(201.3).DP(201.3).02P(201.3).03P(201.3).V(201.3).DV(201.3)
     1,C1,C2,C3,C4,U0(3),AL,BE,CW,R,DELY,C,K,XM
      COMPLEX V00, V10, V20, V30, U00, U10, FK1, GK1, V01, V11, V21, V31, U01, U11,
     1 FK2,GK2,V02,V12,V22,V32,U02,U12,FK3,GK3,FK,GK,FKP,GKP,GK2P,GK3P,
     2 P.DP, D2P, D3P, V, DV, U1, U2, U0, CW, C1, C2, C3, C4, A1, A2, A3, A4, A6, A7, A9
C
         CALCULATE THE REQUIRED VELOCITY AND MAGNETIC QUANTITIES
      CALL VCAL (Y, HM, RM, W, WP, WPP, T, TP, TPP)
      Y=Y+DELY/2.0
```

CALL VCAL (Y,HM,RM,Z,ZP,ZPP,S,SP,SPP)

```
Y=Y+DELY/2.0
      CALL VCAL (Y, HM, RM, U, UP, UPP, H, HP, HPP)
     DO 301 [=1.3
         FUNCTIONS AT Y
C
      V00=P(J,I) $ V10=C+DP(J,I) $ V20=C+C+D2P(J,I)/2.
      V30=C+C+C+D3P(J,1)/6. $ U00=V(J,1) $ U10=C+DV(J,1)
     FK1=((C2+(W-CW)+K)+U00-C2+T+V00-RM+V10/C)+C+C/2.0
      GK1=((C3+(W-CW)+2.+K+XM)+2.+V20/(C+C)+C4+T+2.+V10/C-(C3+K+(W-CW)
     1+C3+WPP+K+K+AL+AL+T+T+XM-C4+TP)+VOO-C4+(W-CW)+U1O/C+(AL+AL+XM+T
     2*(W-CW)-C4*(WP-TPP/RM))*U00)*C**4/24.
С
         FUNCTIONS AT Y+DELY/2.
      V01=V00+0.5*V10+0.25*V20+0.125*V30+0.0625*GK1
      V11=V10+V20+0.75*V30+0.5*GK1 $ V21=V20+1.5*V30+1.5*GK1
      V31=V30+2.0*GK1 $ U01=U00+0.5*U10+0.25*FK1 $ U11=U10+FK1
     FK2=((C2*(Z-CW)+K)*U01-C2*S*V01-RM*V11/C)*C*C/2.0
      GK2=((C3*(Z-CW)+2.*K+XM)*2.*V21/(C*C)+C4*S*2.*V11/C-(C3*K*(Z-CW)
     1+C3+ZPP+K+K+AL+AL+S+S+S+XM-C4+SP)+V01-C4+(Z-CW)+U11/C+(AL+AL+XM+S
     2*(Z-CW)-C4*(ZP-SPP/RM))*U01)*C**4/24.
C
         FUNCTIONS AT Y+DELY
      V02=V00+V10+V20+V30+GK2 $ V12=V10+2.0*V20+3.0*V30+4.0*GK2
      V22=V20+3.0*V30+6.0*GK2 $ V32=V30+4.0*GK2
      U02=U00+U10+FK2 $ U12=U10+2.0+FK2
     FK3=((C2*(U-CW)+K)*U02-C2*H*V02-RM*V12/C)*C*C/2.0
      GK3=((C3*(U-CW)+2.*K+XM)*2.*V22/(C*C)+C4*H*2.*V12/C-(C3*K*(U-CW)
     1+C3*UPP+K*K+AL*AL*H*H*XM-C4*HP)*VO2-C4*(U-CW)*U12/C+(AL*AL*XM*H
     2"(U-CW)-C4*(UP-HPP/RM))*U02)*C**4/24.
      FK=(FK1+2.0*FK2)/3.0 $ FKP=(FK1+4.0*FK2+FK3)/3.0
      GK=(8.*GK1+8.*GK2-GK3)/15. $ GKP=(9.*GK1+12.*GK2-GK3)/5.
     GK2P=2.*GK1+4.*GK2 $ GK3P=(GK1+4.*GK2+GK3)*2./3. $ L=J+1
С
         VALUES OF FUNCTION AND ITS DERIVATIVES AT Y+C
      P(L,I)=V00+V10+V20+V30+GK $ DP(L,I)=(V10+2.*V20+3.*V30+GKP)/C
      D2P(L+1)=(V20+3.*V30+GK2P)*2./(C*C)$D3P(L+1)=(V30+GK3P)*6./(C*C*C)
      V(L,I)=U00+U10+FK $ DV(L,I)=(U10+FKP)/C
C
         CALCULATE SOLUTION TO INVISIO EQN TO BE USED FOR FILTERING
      UO(!)=((U-CW)*(D2P(J+1,1)-K*P(J+1,1))-UPP*P(J+1,1))*AL*C1*R
         DETERMINE GROWING SOLUTION
      IF(J-1) 604,603,604
  603 IF(1-3) 604,599,604
  599 CONTINUE
      DO 302 M=1.3
      AA=REAL(DP(L,M)+(CONJG(DP(L,M))))
      BB=REAL(P(L,M)*(CONJG(P(L,M))))
  302 G(M)=SQRT(AA/BB)
      G1=AMAX1(G(1),G(2),G(3))
      IF(G1.EQ.G(1)) GO TO 604 $ IF(G1-G(2)) 606,605,606
  605 M=2 $ GD TO 607
  606 M=3
  607 DO 608 N=J,L
      A1=P(N,M)   P(N,M)=P(N,1)   P(N,1)=A1
      A2=DP(N,M) S DP(N,M)=DP(N,1) S DP(N,1)=A2
      A3=D2P(N,M)    D2P(N,M)=D2P(N,1)    D2P(N,1)=A3
      A4=D3P(N,M) $ D3P(N,M)=D3P(N,1) $ D3P(N,1)=A4
```

```
A6=V(N,M) $ V(N,M)=V(N,1) $ V(N,1)=A6
A7=DV(N,M) $ DV(N,M)=UV(N,1) $ DV(N,1)=A7
IF(N-J) 400,400,608
400 A9=U0(M) $ U0(M)=U0(1) $ U0(1)=A9
608 CONTINUE
604 CONTINUE
301 CONTINUE
RETURN
END
```

SUBROUTINE VCAL (Y, HM, RM, U, UP, UPP, H, HP, HPP) C THIS SUBROUTINE CALCULATES THE VELOCITY AND INDUCED Ċ MAGNETIC FIELD QUANTITIES AND THEIR DERIVATIVES AT THE REQUIRED Y STATIONS CDSH(X) = (EXP(X) + EXP(-X))/2.0SINH(X) = (EXP(X) - EXP(-X))/2.0C=COSH(HM) \$ S=SINH(HM) IF(Y) 32,31,31 32 Y=-Y \$ CY=COSH(HM#Y) \$ SY=-SINH(HM#Y) \$ Y=-Y \$ GO TO 30 31 CY=COSH(HM*Y) \$ SY=S1NH(HM*Y)30 CONTINUE D=HM*C-S \$ U=HM*(C-CY)/D \$ UP=-HM*HM*SY/D \$ UPP=-HM**3*CY/0 45 H=RM/HM*(SY-Y*S)/(C-1.) \$ HP=RM/HM*(HM*CY-S)/(C-1.) HPP=RM#(HM#SY)/(C-1.) RETURN END

DATA CARDS

1 1 13 10 0.01 0.01 0.01 0.2 1.E-12 1.15 190000. .178 0.0 0.0 6.0 1.E-2

